[14] Low-Noise Patch-Clamp Techniques

By RICHARD A. LEVIS and JAMES L. RAE

Introduction

It has now been more than 20 years since the patch-clamp technique was introduced.[1] However, it was not until the discovery[2,3] that application of suction to the interior of a clean heat-polished pipette pressed gently against the membrane of certain cells often resulted in formation of a membrane–glass seal with a resistance measurable in gigohms (10^9 Ω) that the technique gained wide acceptance. The high resistance of such a seal (commonly called a "gigaseal") resulted in dramatic reductions of background noise levels and sparked an intense period of methodological investigation that developed electronic and electrode technology to take full advantage of the possibilities offered by the gigaseal (see, e.g., Refs. 4–6). In a relatively short period of time following the discovery of the gigaseal the patch-clamp technique quite literally revolutionized the investigation of membrane electrophysiology. A variety of "configurations" were discovered almost immediately, that is, on-cell patches, excised patches of both inside-out and outside-out configuration, and the whole-cell configuration.[4] Refinements in electronics (see, e.g., Refs. 4–6) were also very rapid, leading to patch-clamp amplifiers with noise levels that at the time were adequate to take advantage of the existing pipette technology. Since then progress in patch-clamp electronics has been more gradual, but steady improvements in both noise levels and convenience of use have continued.

Initially it was believed that only certain types of glass and certain cells were suitable for the patch-clamp technique. However, it was rapidly realized that just about any glass pulled into appropriate pipettes could form gigaseals with just about any type of cell (provided only that reasonable access to the cell membrane is available). Rae and Levis[6,7] studied a variety

[1] E. Neher and B. Sakmann, *Nature* **260,** 799 (1978).
[2] F. J. Sigworth and E. Neher, *Nature* **287,** 447 (1980).
[3] E. Neher, *in* "Techniques in Cellular Physiology" (P. F. Baker, ed.) p. 1. Elsevier, Amsterdam, 1982.
[4] O. P. Hamill, A. Marty, E. Neher, B. Sakmann, and F. J. Sigworth, *Pflugers Arch.* **391,** 85 (1981).
[5] F. J. Sigworth, *in* "Single Channel Recording" (B. Sakmann and E. Neher, eds.), 2nd Ed., p. 95. Plenum, New York and London, 1995.
[6] J. L. Rae and R. A. Levis, *Mol. Physiol.* **6,** 115 (1984).
[7] J. L. Rae and R. A. Levis, *Methods Enzymol.* **207,** 66 (1992a).

0076-6879/98 $25.00

of different glasses in order to select those that would produce the lowest noise. As expected, it was found that glasses with the least dielectric loss produced the lowest noise. No major differences were ever clearly demonstrated in the ability of different glasses to form seals. It was clear from these early studies that quartz would be ideal for the fabrication of low-noise patch pipettes. However, quartz softens at 1600° and it was not until 1992 that it became possible to pull conveniently quartz patch pipettes. The use of quartz pipettes[8] and other strategies for reducing pipette noise[9,10] have now demonstrated that the noise of even the most modern electronics can dominate total noise in the best of measurement situations.

This article focuses on noise performance in patch and whole-cell voltage clamping. Background noise arises from a variety of different sources, each of which has to be understood if it is to be effectively minimized. Ultimately, the level of background noise determines what size and duration signals can be resolved by these techniques. Low noise is required to allow filter bandwidth to be increased with the resulting increase in time resolution. Most noise sources in the patch-clamp technique are uncorrelated, which means that they add in an rms (root mean square) fashion. This means that the largest individual noise source or sources can often dominate total noise. Nevertheless, low-noise recordings require attention to just about every detail of the technique. Following a brief introduction to some of the basics of the patch-clamp technique, such details are the major part of this article.

Some Patch-Clamp Basics

Pipettes

The appropriate fabrication of patch pipettes is of central importance to many different aspects of the patch-clamp technique. These include seal formation, the expected size of patch, the quality (resistance, stability) of the seal, and, of course, the background noise levels that can be achieved. The general procedures for fabricating patch pipettes have been described elsewhere[7,11] and are not presented here. Instead we briefly review some of the basic features of pipettes that are most important to performance.

[8] R. A. Levis and J. L. Rae, *Biophys. J.* **65,** 1666 (1993).
[9] J. L. Rae and R. A. Levis, *Pflugers Arch.* **42,** 618 (1992b).
[10] K. Benndorf, *in* "Single Channel Recording" (B. Sakmann and E. Neher, eds.), 2nd Ed., p. 129. Plenum, New York and London, 1995.
[11] A. Cavalie, R. Grantyn and H. D. Lux, *in* "Practical Electrophysiological Methods" (H. Kettenmann and R. Grantyn, eds.), p. 171. Wiley-Liss, New York, 1992.

The first issue that the experimenter must resolve is the type of glass to be used. Quartz is the best selection for very low noise measurements, but using it is expensive. A few other low-loss glasses are readily available, and, although their dissipation factors are much higher than that of quartz, these can produce very good results in many situations. For whole-cell measurements the electrical characteristics of the glass are less important, although there is no need these days to ever use very lossy glasses such as the soda-lime glasses that were once very popular. All pipettes require a coating with a suitable elastomer for low-noise applications. This may sometimes seem unnecessary in some whole-cell situations. Nevertheless, we believe that even in such cases applying a light elastomer coating is a good habit to form. Many different geometries of pipettes have been used. The purpose of these variations has sometimes been to reduce noise and at other times to promote the formation of desirable seals, appropriate patch size, and acceptable access resistance (in whole-cell or giant-patch situations). One of the geometrical considerations that must be addressed is the ratio of the outer diameter (d_o) to inner diameter (d_i) of the tubing used prior to pulling. In terms of noise, large d_o/d_i ratios are usually desirable in small patch measurements, whereas smaller d_o/d_i ratios may be better selections for whole-cell recording, since these make it easier to produce low-resistance pipettes. Heat polishing of pipettes can be used to great advantage in many situations; this is particularly true when making whole-cell or large patch measurements. However, it has been shown for quartz pipettes (where heat polishing is impractical due to the high melting temperature of quartz) and for very small tipped pipettes made from quartz or other glasses (where visualization of the tip becomes difficult or impossible) that seals can readily be formed without heat polishing. Issues concerning pipette noise are considered extensively in this article.

Seal Formation

Of course the formation of a high-resistance membrane–glass seal is a prerequisite for low-noise patch-clamp recordings. A high-resistance seal dramatically reduces background noise and enhances recording stability. The mechanisms involved in seal formation are not completely understood (although ideas have been proposed). Thus empirical information based on experience has guided efforts to form efficiently the highest resistance and most stable seals possible. In general, the pipette is pressed against the surface of the selected cell until a noticeable (about a factor of 1.5–2 is typical) change in resistance of the pipette occurs. Pipette resistance is usually monitored by applying a small periodic square-wave potential to the pipette and measuring the resulting current; many software packages

for patch clamping have automated this procedure to provide a rapidly updating digital readout of resistance. On occasion seals will form spontaneously when the pipette presses against the cell membrane. More often, however, suction must be applied to the interior of the pipette. A gigaseal will then usually form, although the process may be sudden or gradual (requiring up to about 30 sec). It is generally found that smaller tipped pipettes form higher resistance seals, although there is a great deal of scatter in the value of seal resistances even among apparently identical pipettes. High-resistance seals (e.g., >50 GΩ) are very important to achieving low-noise measurements, and it is to be expected that the higher the seal resistance the lower the noise attributable to the seal will be. Seal noise is difficult to study and has never been characterized in great detail. The noise of the seal is most important at relatively low bandwidths. Thus a 10 GΩ seal may be adequate if you plan to record at bandwidths of 20 kHz or more, while a seal well in excess of 100 GΩ is often desirable when recording at bandwidths of less than 1 kHz.

Configurations

Cell-Attached Patch. The first and most basic configuration is the cell-attached patch. In this configuration a seal is formed with the cell and a membrane patch is thus isolated. Clearly the rest of the cell is then in series with the patch membrane (i.e., patch currents must flow through the rest of the cell membrane). This is not a problem in most situations, but could occasionally produce unwanted effects (e.g., when measuring fairly large currents in a patch on a very small cell). In addition, the on-cell patch does not allow you to know accurately the transpatch potential because of the unknown cell membrane resting potential. Finally, this configuration does not allow changing the ionic composition on both sides of the patch membrane. Thus cell-attached recordings are most commonly used when the channel being studied requires some unknown cytoplasmic factor or factors for normal gating; such factors would be lost if the patch was excised from the cell.

Excised Patches. Excised patches allow easy access to one side of the patch and allow precise control of the transpatch potential. Such patches are also the best choice for very low noise recording since they can readily be withdrawn toward the surface of the bath minimizing immersion depth. There are two basic types of excised patches.

Inside-Out Patches. Inside-out patches are easily formed by simply withdrawing the pipette from the cell surface after a seal has been formed. This configuration allows easy access to the intracellular side of the membrane. The most common difficulties associated with inside-out patches are

the loss of cytoplasmic factors that may be involved in modulating behavior of some channels and the possibility that a closed vesicle may form.[4]

OUTSIDE-OUT PATCHES. Outside-out patches are formed by disrupting the patch membrane after a seal has been formed and then withdrawing the pipette slowly from the cell surface. In most cases a new patch will be formed with the outer membrane surface facing the bath. This allows easy access to the extracellular face of the patch membrane. As was the case in inside-out patches the loss of cytoplasmic factors affecting some channels may be a problem. In addition, there is no way of knowing before excision what the patch will contain since the original patch with its channels has been destroyed. Finally, in our experience forming stable outside-out patches for high-quality measurements is somewhat more difficult than forming inside-out patches.

Whole-Cell Recording. Whole-cell recording is a powerful technique for measuring the currents from an entire cell. This configuration is normally easily obtained after a seal has been formed by disrupting the patch membrane with additional suction or a brief large voltage pulse. An alternative method is the perforated patch technique.[12,13] A possible shortcoming of the "traditional" whole-cell technique in some situations is the loss of cytoplasmic factors from the cell interior; this can usually be avoided by the perforated patch approach to whole-cell measurements. It is also common to find that the access resistance measured after patch disruption (or perforation) is higher than the original resistance of the pipette. Series resistance compensation is often very important when currents are large or wide bandwidth recordings are desired.

Giant Patches. Gigaseal formation becomes progressively less likely as the size of the pipette tip increases. However, application of a hydrocarbon coating to the pipette tip enhances seal formation and has allowed the formation of patches with diameters in the range of 10–40 μm with patch capacitances of 2–15 pF and seal resistances in the range of 1–10 GΩ.[14,15] Giant patches can be formed in both cell-attached and excised configurations. The noise of such patches is likely to be dominated at high frequencies by the thermal voltage noise of the pipette in series with the large patch capacitance and at lower frequencies by the relatively low seal resistances usually obtained (plus any noise associated with the membrane itself). However, in most cases relatively large signals are expected from such

[12] R. Horn and A. Marty, *J. Gen. Physiol.* **92,** 145 (1988).
[13] J. L. Rae, K. Cooper, P. Gates, and M. Watsky, *J. Neurosci. Methods* **37,** 15 (1991).
[14] D. W. Hilgemann, *Pflugers Arch.* **415,** 247 (1989).
[15] D. W. Hilgemann, *in* "Single Channel Recording" (B. Sakmann and E. Neher, eds.), 2nd Ed., p. 307. Plenum, New York and London, 1995.

patches and thus the signal-to-noise ratio can remain very favorable for many measurements.

Electronics

Patch-clamp electronics have been described in detail in many previous publications by ourselves and others (see e.g., Refs. 5, 6, and 16) and these details are not repeated here. Instead only a few comments that relate to the material of this paper are summarized.

Headstage Amplifier. The "headstage" amplifier is the most important part of the patch clamp in terms of noise. Two basic varieties are available from several manufacturers, namely, resistive feedback headstages and capacitive feedback headstages. Capacitive feedback offers lower noise and can produce wider bandwidth. The noise of a specific capacitive feedback amplifier is described in detail later. Many amplifiers contain two or more different feedback elements for different situations. Capacitive feedback or very high valued resistive feedback (typically 50 GΩ) is intended for small patch measurements and provides the lowest noise. Lower valued resistors are provided for whole-cell situations (typically 500 MΩ for cells of up to 100 pF and 50 MΩ for larger cells) and might also be used with large patches. The noise of the headstage with a 500-MΩ feedback resistor is considerably higher than that with a 50-GΩ resistor or capacitive feedback.

Capacity Compensation. Capacity compensation is provided to cancel transients resulting from the charging of the capacitance of the pipette and its holder (plus other sources of capacitance at the headstage input) when the potential is changed. Most patch clamps provide two time constants to cancel such transients. The second slower time constant is primarily needed to deal with the lossy capacitance of glass pipettes. We have shown that this component is smallest in low-loss glasses.[7] The slow component is *not* well described by a single exponential and therefore cannot be completely canceled by the compensation circuits provided in commercial patch clamps. Minimization of this component is therefore best accomplished by using low-loss glasses (soda-lime glasses in particular should be avoided) and coating pipettes with low-loss elastomers; quartz produces the least amount of such a slow component. For low-noise applications minimization of capacitance is very important. Note also that in addition to the noise arising from the capacitance at the headstage input, the capacity compensation circuitry can also add noise of its own.

Whole Cell Compensations. When performing whole-cell measurements series resistance compensation is often very important. This is discussed in

[16] R. A. Levis and J. L. Rae, *Methods Enzymol.* **207,** 18 (1992).

some detail later. In addition to series resistance compensation, commercial patch-clamp amplifiers also provide compensation for the whole-cell capacitance. This is important in eliminating transients when membrane potential is changed. Of course, the capacitance of the pipette (etc.) also needs to be compensated in this situation.

Low-Noise Recording Techniques

Noise in Single-Channel Measurements

Overview of Patch-Clamp Noise. The noise associated with single-channel patch-clamp measurements has a power spectral density (PSD) that can generally be described by

$$S_{pc}^2 = a_0/f + a_1 + a_2 f + a_3 f^2 \qquad \text{amp}^2/\text{Hz} \tag{1}$$

where a_0, a_1, a_2, and a_3 are coefficients that describe the contribution of each noise term to total noise power and f is the frequency in hertz. The rms noise resulting from this PSD can be obtained by integrating from a low-frequency cutoff of B_0 to a high-frequency cutoff of B (Hz) and taking the square root of the result. This yields:

$$I_{pc} = (c_0 a_0 \ln(B/B_0) + c_1 a_1 B + c_2(a_2/2)B^2 + c_3(a_3/3)B^3)^{1/2} \qquad \text{amp rms} \tag{2}$$

where c_0, c_1, c_2, and c_3 are coefficients that depend on the type of filter used, and it has been assumed that $B \gg B_0$ [so that B_0 has been ignored in the last three terms of Eq. (2)]. The coefficient c_0 can usually be taken to be 1.0 without introducing too much error. In considering $1/f$ noise it is more important to determine B_0, the effective low-frequency cutoff of the measurement. Because high-pass filters are not used in most single-channel measurements, B_0 must instead be deduced on the basis of the duration of the measurement (the longer the duration, the smaller B_0). The other coefficients, c_1, c_2, and c_3, need further explanation. For a "brickwall" filter (i.e., a filter that rolls off extremely rapidly at frequencies above its corner frequency) these coefficients are all essentially 1.0. However, for filters with desirable time-domain characteristics the coefficients are larger than 1.0. For an eight-pole Bessel filter (which is the most commonly used type for time domain measurements) these coefficients are approximately $c_1 \approx 1.05$, $c_2 \approx 1.3$, and $c_3 \approx 2.0$.

From Eqs. (1) and (2) it can be seen that patch-clamp noise PSD is generally described by terms that include white noise and terms that vary with frequency as $1/f$ (more precisely $1/f^{\alpha}$ where α is usually near 1.0), f,

and f^2. These terms give rise to terms that contribute to total rms noise in proportion to $[\ln(B/B_0)]^{1/2}$, $B^{1/2}$, B, and $B^{3/2}$.

The $1/f$ noise arises from the patch-clamp amplifier and possibly from the seal and the patch itself; in many situations $1/f$ noise can be neglected in that its contribution to overall noise is often very small. White noise arises from the patch-clamp amplifier, from the seal, and from the patch membrane. The f noise arises primarily from lossy dielectrics; these include aspects of the patch-clamp amplifier, and (usually more importantly) the pipette and its holder. The f^2 current noise arises from voltage noise (white) in series with a capacitance. There are several sources of this type of noise in typical patch-clamp recording situations; these include the patch-clamp amplifier, capacitance added to the amplifier input by the holder and pipette, distributed RC noise, and noise arising from the pipette resistance in series with the patch capacitance (R_c-C_p noise).

Clearly $1/f$ noise is most important when bandwidth is very limited (e.g., in the measurement of very small currents) and it generally sets the limit on how much noise may be reduced by restricting bandwidth. White noise is also most important at relatively low bandwidths. Noise types f and particularly f^2 become progressively more important as bandwidth increases.

It is important to note that most noise sources involved in patch-clamp measurements are uncorrelated. This means that they will add together in an rms fashion; that is, considering three uncorrelated noise sources contributing to total noise with rms values in a particular bandwidth denoted by e_1, e_2, and e_3, total rms noise (e_T) is then given by

$$e_T = (e_1^2 + e_2^2 + e_3^2)^{1/2} \tag{3}$$

An important aspect of this is that the largest individual source of noise can dominate total noise. Thus if $e_1 = 2$ and both e_2 and $e_3 = 1$, then $e_T = 2.45$, which is only 22% more than e_1 alone. This type of information must be remembered when judging the importance of various noise sources in different situations and in determining appropriate compromises between different types of noise when this is required.

The theoretical aspects of individual noise sources are now described beginning with the patch-clamp headstage amplifier.

Patch-Clamp Amplifier. The first noise source to consider is that of the patch-clamp amplifier itself. Considerable progress has been made in recent years to reduce the noise of patch-clamp electronics for single-channel measurements. This has been primarily due to the introduction of capacitive feedback amplifiers; such amplifiers are now available from several manufacturers. Prior to the use of capacitive feedback, patch-clamp amplifiers relied on high-valued resistors as the feedback element; for single-channel

measurements the use of a 50-GΩ resistor has been the most common selection. A variety of disadvantages to such resistors have been described elsewhere.[7,16] Briefly, such resistors have a very limited frequency response and thus require "boost" circuits[5,6] to restore the high-frequency components of the measured signal (and, of course, of the noise). Often the frequency response is not characterized by a simple one-pole *RC* rolloff, necessitating complex boost circuits and/or less than perfect corrected responses. Boost circuits need to be retuned periodically because the characteristics of the resistor may vary somewhat over time. In addition, high-valued resistors sometimes show relatively high voltage and temperature coefficients of resistance (i.e., resistance changes slightly with temperature and the voltage across the resistor). This can lead to nonlinearities and small changes of the boosted response with changes in temperature and signal amplitude. Nevertheless, adequate dynamic performance can be achieved with usable bandwidths in excess of 30 kHz. However, more importantly for the present discussion, all high-valued feedback resistors currently available that we are aware of display considerably higher noise than simply the expected thermal current noise.[7,16] The result of all this is that resistive feedback amplifiers typically display open-circuit noise of about 0.25-pA rms in a 10-kHz bandwidth (eight-pole Bessel filter). Capacitive feedback amplifiers can have as little as about half this much noise.

The amplifier that we use for low-noise measurements is the Axopatch 200B (Axon Instruments, Foster City, CA). We deal specifically with one of these instruments and its noise in this discussion so that examples later in the chapter can be associated with specific numerical values. However, the principles described also apply to other amplifiers of this general type made by this and other manufacturers. The input referred open-circuit noise PSD, S_{hs}^2, of the instrument used by one of us is very well fit by the following equation:

$$S_{hs}^2 = 1.9 \times 10^{-32} + 3.5 \times 10^{-35} f + 1.3 \times 10^{-38} f^2 \qquad \text{amp}^2/\text{Hz} \quad (4)$$

where f is the frequency in hertz. This was the lowest noise instrument of the first 10 or so manufactured. The noise PSD is adequately described by a white noise component and components that rise with increasing frequency as f and f^2. This amplifier displays very little $1/f$ current noise, and whatever amount is present is difficult to quantify since it requires very long measurement times and is thus subject to interference arising from mechanical vibrations (and periodic resets). The maximum value of any $1/f$ current noise component of the open-circuit amplifier PSD is $\sim 2 \times 10^{-32}/f$, indicating a $1/f$ corner frequency of about 1 Hz or less.

The white noise term of Eq. (4) is equivalent to the thermal voltage noise of an 850-GΩ resistor; it arises from the shot noise of the input

junction field effect transistor (JFET) and from noise associated with the differentiator, which follows the integrating headstage amplifier. In fact, the differentiator is the largest contributor to this noise, producing about $1.1–1.2 \times 10^{-32}$ amp^2/Hz.[17] The JFET in the Axopatch 200B is cooled to about $-20°$ and its gate leakage current can be calculated to be about 0.02 pA, contributing about 7×10^{-33} amp^2/Hz to the white noise term.

The f noise component of Eq. (4) arises primarily from lossy dielectrics associated with the input; these dielectrics include packaging, capacitors, and some contribution from the JFET itself (quite possibly associated with the surface passivation layer). A small contribution to this term arises from $1/f$ voltage noise of the input JFET in series with capacitance associated with the input. The f^2 noise term of Eq. (1) arises primarily from the white noise component of the input voltage noise of the JFET in series with the capacitance associated with the input. This capacitance is dominated by the input capacitance of the JFET itself, but also includes strays, the feedback capacitor and the capacitor used to inject compensation signals, and capacitance associated with the input connector. Smaller contributions to this term arise from noise associated with compensation signals and a term arising from the differentiator.

Equation (4) can be integrated over a bandwidth (i.e., DC to B Hz) to provide an equation for the variance as a function of frequency. The square root of this result is the input referred rms noise of the open-circuit amplifier (here called i_{hs}) as a function of bandwidth:

$$i_{hs} = (1.9 \times 10^{-32} c_1 B + 1.75 \times 10^{-35} c_2 B^2 + 4.3 \times 10^{-39} c_3 B^3)^{1/2} \text{ amps rms} \quad (5)$$

where c_1, c_2, and c_3 are coefficients that depend on the type of filter used. As mentioned previously, for an eight-pole Bessel filter these are approximately $c_1 \approx 1.05$, $c_2 \approx 1.3$, and $c_3 \approx 2.0$.

Thus this particular amplifier has open-circuit noise of approximately 7-, 41-, and 105-fA rms in bandwidths of 1, 5, and 10 kHz (eight-pole Bessel filter), respectively.

Most noise sources encountered in actual patch-clamp recordings are uncorrelated and therefore simple rules of rms addition apply [see Eq. (3)]. However, this is not the case with noise arising from the input voltage

[17] The noise contribution of the differentiator can be changed by changing its feedback resistor. This will also change the overall gain and bandwidth of the integrator/differentiator combination. For example, increasing the feedback resistor by a factor of 10 will increase the gain by the same factor and decrease the available bandwidth by a factor of 3.16 ($10^{1/2}$). The PSD of the white noise contribution will fall by a factor of 10. Decreasing the feedback resistor will have the opposite effect—decreased gain, increased bandwidth, and increased differentiator noise contribution.

noise, e_n, of the JFET and capacitance added to the input by the addition of the holder and pipette. This noise is perfectly correlated with noise arising from other capacitance at the input (JFET capacitance, strays, feedback and injection capacitors, capacitance of the input connector) so the usual rules of rms addition of uncorrelated noise sources do not apply in this case. This noise has a PSD that rises as f^2 and adds to the f^2 term of Eq. (4). The addition of 2 pF of capacitance (a reasonable number for a small holder and pipette with a moderate depth of immersion) at the input will increase this term to approximately $1.9 \times 10^{-38} f^2$ amp^2/Hz, and this in turn would increase the rms noise of the particular headstage considered here in bandwidths of 5 and 10 kHz (eight-pole Bessel filter) to 47- and 123-fA rms, respectively. Obviously less capacitance will lead to smaller increases in noise and more capacitance would lead to larger noise increments. Remember that the holder and pipette will also contribute other types of uncorrelated noise (see later discussion). However, we will include in the noise of the headstage the noise arising from e_n and *all* capacitance at the input, including the capacitance of the holder and pipette.

Holder Noise. The addition of a traditional holder to the headstage input adds noise due to its capacitance in series with e_n as just described, and because of the lossiness of this capacitance. The lossy capacitance adds *dielectric noise.* The magnitude of this noise is dependent on the size and geometry of the holder and on the material from which the holder is constructed. The most important parameter of the holder material is its dissipation factor. In general a capacitance, C_d, with a dissipation factor D will produce dielectric noise with a PSD, S_d^2, given by

$$S_d^2 = 4kTDC_d(2\pi f) \qquad \text{amp}^2/\text{Hz} \tag{6}$$

where k is the Boltzmann constant and T is absolute temperature. Over a bandwidth of B Hz this will produce an rms noise current given by

$$i_d = (4kTDC_d c_2 \pi B^2)^{1/2} \qquad \text{amp rms} \tag{7}$$

The best materials commonly used to fabricate pipette holders are polycarbonate and Teflon. Teflon has a lower dissipation factor ($\sim 2 \times 10^{-4}$), but displays piezoelectric and space charge effects. The dissipation factor of polycarbonate is higher ($\sim 10^{-3}$), but in actual practice either material has produced acceptable results. Lucite holders should be avoided for low-noise measurements because the dissipation factor of Lucite is rough 30–40 times higher than that of polycarbonate.

As described by Levis and Rae,[8] precise calculations of the dielectric noise introduced by a pipette holder are complicated by the rather complex equivalent circuit presented by most holders. Rough calculations have indicated that a small polycarbonate holder with a capacitance of 0.6 pF is

predicted to produce approximately 15-fA rms noise in a bandwidth of 5 kHz; a larger holder (measured capacitance ~1.5 pF) should produce about 25-fA rms noise in this bandwidth. These numbers are in good agreement with actual measurements of holder noise. With a small polycarbonate holder attached to the headstage considered here, noise increases to about 46-fA rms in a 5-kHz bandwidth (eight-pole Bessel filter). A 1.5-pF polycarbonate holder should increase this value to about 52-fA rms.

Benndorf[10] has reported the use of a metal body pipette holder of very small size. Such a holder will not produce significant dielectric noise, but will only slightly add to the capacitance (almost lossless) at the headstage input. Benndorf does not report the amount of capacitance added by this holder, but its size suggests that it is a very small increment. This design doubtlessly represents the lowest noise possible from a holder, but given the small increment in noise associated with more traditional holders and the moderate amount of inconvenience that seems to be associated with the use of the tiny metal holder (and extremely short pipettes fixed with wax to the holder), its utility is not clear except in the most demanding of applications. Benndorf[10] also reports $1/f$ noise associated with polycarbonate holders; we have not found any significant amounts of such noise in the holders that we use.

Note that it is imperative to keep holders clean to achieve the low-noise levels described.

Pipette Noise. The noise associated with pipettes has been discussed extensively in previous publications by ourselves and others.[7,8,10,16] The following review adds only a few new features to the theoretical aspects of pipette noise, although dielectric noise and particularly distributed RC noise are considered in greater detail than in the past, refining and in some cases modifying previous conclusions. This article attempts to bring together a wide range of theoretical and practical information concerning pipette noise in a convenient format.

Several different mechanisms contribute to the noise arising from the pipette. Figure 1 shows a simplified circuit representation of the four most important noise mechanisms resulting from the pipette per se. We first summarize all pipette noise sources and then describe the most important of these in greater detail. Both theoretical and practical issues relating to noise minimization are considered.

1. The pipette adds capacitance to the input of the amplifier. This depends on the length of the electrode, its geometry (especially wall thickness), the use of elastomer coatings, and the depth of immersion. This capacitance is in series with e_n and produces f^2 noise by the mechanism described earlier.

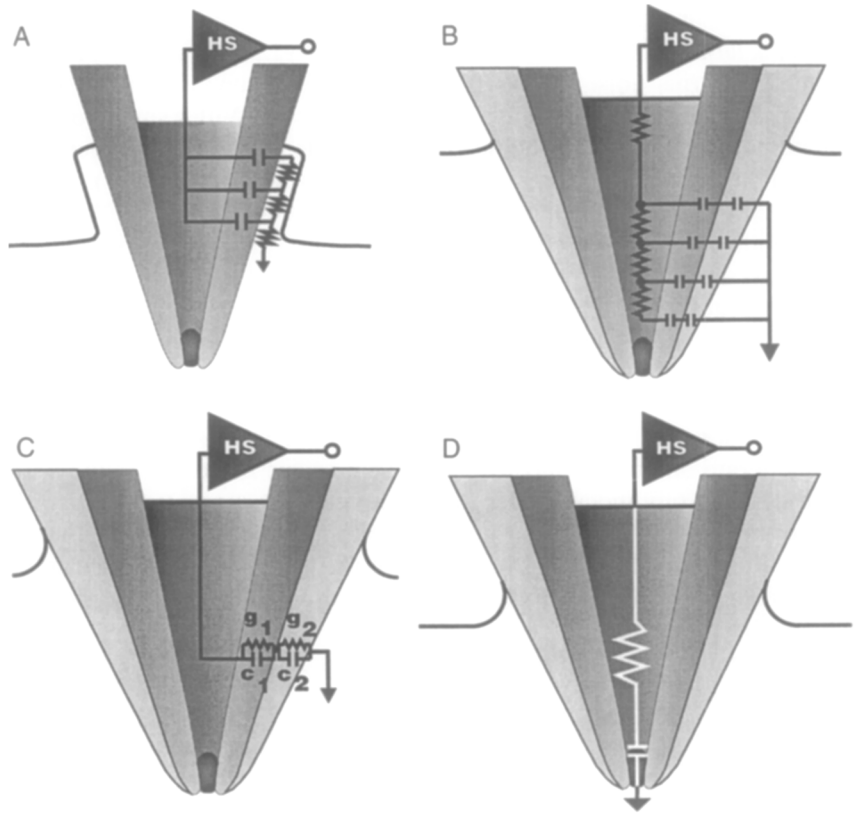

FIG. 1. Simplified circuit representation of the four most important noise mechanisms associated with the patch pipette per se. (A) Thin-film noise arising from the thermal voltage noise of the distributed resistance of a thin film of solution on the pipette exterior in series with the capacitance of the pipette wall. Similar films may also form within the pipette and in the holder. Note that in part (A) the pipette is shown without an elastomer coating; such a coating can essentially eliminate exterior thin film noise. In parts (B), (C), and (D) the pipette is shown with an elastomer coating. (B) Distributed *RC* noise arising from the thermal voltage noise of the distributed resistance of the pipette filling solution in series with the distributed wall capacitance of the immersed portion of the pipette. (C) Dielectric noise of an elastomer coated pipette arising from the series combination of the glass pipette itself (g_1, C_1, where $g_1 = \omega C_1 D_1$, $\omega = 2\pi f$) and the elastomer (g_2, C_2, where $g_2 = \omega C_2 D_2$). (D) R_c-C_p noise arising from the thermal voltage noise of the entire pipette resistance in series with the capacitance of the patch. This figure does not include noise arising from the pipette capacitance in series with the input voltage noise, e_n, of the headstage amplifier, or noise associated with the seal. See text for further details.

2. The capacitance of the immersed portion of the pipette also will produce dielectric noise (Fig. 1C). The amount of this noise depends on the type of glass used, the wall thickness of the glass, the type and thickness of the elastomer coating, and the depth of immersion of the pipette. Dielectric noise produces a PSD that rises linearly with increasing frequency (f noise).

3. Distributed RC noise (Fig. 1B) is the name we use to describe the current noise arising from the thermal voltage noise of the distributed resistance of the pipette filling solution in series with the distributed capacitance of the pipette wall. The capacitance is distributed more or less evenly along the immersed portion of the pipette (assuming a roughly constant ratio of inner to outer diameter of the pipette, see later section). The resistance is primarily located near the tip; however, significant resistance remains in regions distal to the tip. The thermal voltage noise of the distributed pipette resistance in series with the distributed capacitance of the immersed portion of the pipette wall produces noise with a PSD that rises with increasing frequency as f^2 over the range of frequencies of interest to patch clamping. Distributed RC noise is dependent on the geometry of the pipette and the thickness of its walls, the thickness of elastomer coating, the resistivity of the filling solution and the depth of immersion. It is virtually independent of the type of glass used except insofar as this selection affects wall capacitance (primarily due to the dielectric constant of the glass).

4. R_e-C_p noise (Fig. 1D) is the term we use to describe noise arising from the total resistance of the pipette, R_e, in series with the capacitance of the patch, C_p. This noise clearly depends on the value of the pipette resistance and of the patch capacitance. It is usually minimized by using small-tipped pipettes. R_e-C_p noise produces noise that rises as f^2 over the range of frequencies important to patch voltage clamping.

5. Thin-film noise (Fig. 1A) is produced by films of solution that can form on the outer surface of an uncoated pipette as it emerges from the bath. Such a film can have a very high distributed resistance that is in series with the distributed capacitance of the pipette wall. The noise expected from such a film should rise at low to moderate frequencies and then level out at frequencies in the range of kilohertz to tens of kilohertz. Such a thin film can be a very significant source of noise. Fortunately, however, noise from such films on the external pipette surface can be essentially completely eliminated by coating the pipette with a suitable elastomer. Suitable elastomers present a hydrophobic surface that prevents the formation of external films. It is also possible for such films to form inside the pipette or its holder. Such internal films can be prevented by layering a millimeter or so of silicone or paraffin oil on top of the filling solution. However this is not

normally necessary if excess fluid is carefully cleaned from the back of the pipette by suction and (if necessary) drying the pipette with a jet of air. Maintaining the holder free from solutions is very important.

6. Seal noise is probably the least understood source of noise associated with the pipette. It is clearly minimized by the highest possible seal resistance, but in our experience seal noise is often somewhat unpredictable. Seal noise is considered in greater detail later.

The minimization of pipette noise is often relatively straightforward, and often requires only a small amount of additional effort (although it can become expensive if quartz pipettes are selected). Most necessary precautions are simple and reasonably intuitive. Thus, for example, short pipettes are always advantageous, as is the use of thick-walled glass and a heavy coating of a low-loss elastomer as close as possible to the tip. Shallow depths of immersion will minimize noise whenever this is compatible with the experiment being undertaken. Cleanliness is obviously important. In some cases, however, ultimate minimization of noise is not always compatible with a particular type of measurement. For example, very small-tipped pipettes will reduce R_c-C_p noise and tend to produce the highest seal resistance; they also reduce the likelihood of the patch containing charge translocating processes other than those to be measured. Of course, tiny patches also reduce the likelihood of the patch containing the channel to be studied. Thus this strategy is not always appropriate. In the following discussion we attempt to consider both theoretical and practical methods of achieving the lowest possible noise in various situations.

DIELECTRIC NOISE. Dielectric noise results from thermal fluctuations in lossy dielectrics. The magnitude of this noise can be related to the real part of the admittance (the loss conductance) of the dielectric material. Dielectric noise is often the dominant source of noise associated with the pipette. This is particularly true if quartz is not used for pipette fabrication. The equations describing the PSD and rms noise of a single dielectric have already been presented [Eqs. (6) and (7)]. These equations clearly show that dielectric noise depends on the capacitance in question (here the pipette) and on the dissipation factor associated with this capacitance. The dissipation factor and dielectric constant of several glasses are shown in Table I; data for two elastomers are also included. This list is much shorter than lists published previously because many glasses have become scarce or are now completely unavailable. Clearly quartz has the lowest dissipation factor (by a wide margin) and it also has the lowest dielectric constant (by a much smaller margin). Soda-lime glasses (such as 0080) should be avoided for low-noise measurements due to their high dissipation factor and dielectric constant.

TABLE I
DISSIPATION FACTORS AND DIELECTRIC CONSTANTS OF SELECTED GLASSES AND ELASTOMERS

Sample	Dielectric constant	Dissipation factor
Shott 8250	4.9	0.0022
Shott 8330	4.6	0.0037
7740	5.1	0.005
7052	4.9	0.003
Quartz	3.8	10^{-5}–10^{-4}
Soda-lime glass (0080)	7.2	0.009
Sylgard #184	2.9	0.002
R-6101	Not known	0.00025[a]

[a] The dissipation factor listed for R-6101 is an unpublished value provided by the manufacturer; we have not attempted to verify this value in independent tests.

Dielectric noise of the pipette can contribute a large fraction of the total pipette noise, and thus of the noise of the measurement. For example, using Eq. (7), a capacitance, C_d, of 3 pF with a dissipation factor, D, of 0.01 (appropriate for some soda-lime glasses) will produce about 0.22-pA rms noise in a 5-kHz bandwidth. On the other hand, it is certainly possible to minimize dielectric noise. Thus, for example, with C_d of 1 pF and D of 0.0001 (appropriate for quartz), dielectric noise would be only about 13-fA rms in the same bandwidth.

Coating a pipette with a low-loss elastomer such as Sylgard 184 or R-6101 (K. R. Anderson, Santa Clara, CA) will in most cases reduce dielectric noise; quartz is a notable exception to this as described later. Such coating is absolutely necessary for low-noise recordings because it will essentially eliminate thin-film noise and will also reduce distributed RC noise (see later discussion). Of course, the noise of a pipette coated with an elastomer can no longer generally be described by the simple equations presented [Eqs. (6) and (7)] because the coated pipette is the series combination of two different dielectrics (the glass and the elastomer). Levis and Rae[8] have presented equations that describe the noise of two dielectrics in series and described expected and measured results for quartz pipettes in considerable detail. The equation for the rms noise of two dielectrics with capacitances C_1 and C_2 and associated dissipation factors D_1 and D_2 is well approximated by the following if D_1, $D_2 \ll 1$ (as is the case here):

$$i_d = [4kTc_2\pi B^2(D_1C_1C_2^2 + D_2C_2C_1^2)/(C_1 + C_2)^2]^{1/2} \quad \text{amp rms} \quad (8)$$

where B is the bandwidth in Hertz and c_2 is a coefficient that depends on the type of filter used ($c_2 \approx 1.3$ for an eight-pole Bessel filter).

Equation (8) can be used to demonstrate a number of conclusions concerning glass type and elastomer coating and the thickness of both the glass and the coating. In the first place it is useful to consider the expected values of the capacitances in Eq. (8). We consider C_1 and D_1 to represent the glass and C_2 and D_2 to represent the elastomer. The capacitance of a tapering cylinder that preserves the ratio of inner diameter, d_i, to outer diameter, d_0, is proportional to $1/\ln(d_o/d_i)$. This can be used to give a rough estimate of capacitances C_1 (glass) and C_2 (elastomer). For a glass with a dielectric constant of 4 (slightly more than quartz and slightly less than most borosilicates) the capacitance is approximately (0.22 pF/mm)/$\ln(d_o/d_i)$. For an elastomer with a dielectric constant of 3, the capacitance is about (0.17 pF/mm)/$\ln(d_o/d_i)$, where d_o and d_i now refer to only the elastomer coating. Glasses commonly used in patch clamping have d_o/d_i ratios ranging from about 1.2 to 4 or more. These values would produce capacitances ranging from about 1.2 pF/mm of immersion (for $d_o/d_i = 1.2$) to 0.16 pF/mm of immersion (for $d_o/d_i = 4$). Coatings of elastomers can be built up to fairly large thickness, although formation of very thick coats near the tip of the pipette is difficult due to the tendency of the elastomer to flow away from the tip prior to curing (see later discussion). An elastomer coating with $d_o/d_i = 1.5$ (here d_o refers to the outer diameter of the elastomer coat and d_i refers to its inner diameter, which, of course, corresponds to the outer diameter of the glass) would have a capacitance of about 0.4 pF/mm of immersion; for $d_o/d_i = 2$, this would decrease to about 0.25 pF/mm. The general advantages of thick-walled glass and of heavy elastomer coating are thus immediately clear, as is the advantage of shallow depths of immersion. Thick-walled glass, heavy coats of elastomer, and shallow depths of immersion reduce the pipette capacitance. Unfortunately, the numbers just presented are highly approximate because the ratios d_o/d_i of the walls of the pipette near the tip and particularly of the elastomer coating are not uniform. In the case of the pipette, there always appears to be some thinning of the glass near the tip. The extent of such thinning depends on the glass type and more importantly on the geometry to which the glass is pulled. Sharp-tipped pipettes with a small cone angle appear to most closely preserve the d_o/d_i ratio as the pipette is pulled (d_o/d_i ratios at the tip of >95% of the initial tubing ratio have been reported[10]), although not too much thinning can be preserved even with somewhat blunter tipped pipettes. Large-tipped pipettes (prior to fire polishing) with pronounced bullet shapes often produce quite considerable thinning near the tip. Thus the estimates of pipette capacitance listed earlier are generally lower than the actual capacitances observed. For example, with $d_o/d_i = 2$ quartz tubing, pulled to pipettes with roughly a 1-μm tip diameter and a resistance of ~5–10 MΩ, Levis and Rae[8] found that the d_o/d_i ratio decreased to about 1.4–1.5

within about 1 mm of the tip. However, even in such cases the *relative* improvements resulting from thicker walled tubing are more or less as predicted. For elastomer coating the nonuniformity in d_o/d_i is generally even more pronounced; thick coats are easy to build up a few hundred microns back from the tip but are much more difficult to produce near the tip. Levis and Rae[8] have described a method that can produce good results all the way to the tip, but even so there is pronounced thinning of the elastomer in the regions nearest the tip. Thus, as was the case with the glass, the estimates of elastomer capacitance given here should be thought of as simple approximations. Details of variations in wall thickness of the glass and of the elastomer coating are presented for some specific pipette geometries in the discussion of distributed *RC* noise.

The dissipation factors of quartz and several other glasses as well as those of two elastomers are listed in Table I. From this table it is clear that quartz has a dissipation factor that is at least 20–30 times lower than that of any other available glass. Pulling quartz into patch pipettes only became possible after the introduction of a laser-based puller (P-2000, Sutter Instruments, Novato, CA) in 1992. Levis and Rae[8] extensively studied the properties of quartz pipettes and concluded that they were the best selection for ultra-low-noise recordings due to low dielectric noise. These conclusions remain valid at the time of this writing, although it should be noted that the geometry of the pipettes investigated in that study was restricted to relatively blunt tapered pipettes (R_e typically about 5–10 MΩ for a ~1-μm tip diameter) and tubing with d_o/d_i ratios was generally in the range of 1.4–2.0 (although a ratio of 3.0 was used in a few experiments at that time). An important conclusion of that study with regard to dielectric noise was that an elastomer coating generally *increased* the dielectric noise of quartz pipettes, but that heavily coated quartz pipettes still showed significantly less dielectric noise than pipettes fabricated from any other type of glass. Theoretical predictions and actual measurements showed that for quartz pipettes fabricated from tubing with a d_o/d_i ratio of 2, coated with Sylgard 184 all the way to the tip, and immersed in the bath to a depth of ~1.8 mm, dielectric noise attributable to the pipette was about 35-fA rms in a 5-kHz bandwidth. Other measurements suggested that dielectric noise can be as low as 15-fA rms in this bandwidth for similar pipettes with a shallower depth of immersion. We have now occasionally used quartz tubing with $d_o/d_i = 4$ and, particularly with pulling techniques that attempt to preserve this ratio near the tip, we believe that these pipettes can display even less dielectric noise.

Examination of Eq. (8) shows why coating with Sylgard 184 with a dissipation factor of 0.002 will improve the dielectric noise of pipettes fabricated from glasses other than quartz (which have dissipation factors

higher than that of Sylgard), but will actualy increase the dielectric noise of a pipette fabricated from quartz (which has a dissipation factor at least 20 times less than that of Sylgard). For light coats of Sylgard, C_2 (the capacitance of the immersed portion of the elastomer coating) will generally be more than C_1 (the capacitance of the immersed portion of the glass). With heavy coats of elastomer C_2 can become smaller than C_1, although our experience indicates that for glass with an initial d_o/d_i ratio of 2 (and a pulled ratio of ~1.4–1.5 near the tip) that even with the best techniques it is difficult to produce a value of C_2 less than about $C_1/3$ for an immersion depth of ~2 mm. With shallower depths of immersion and/or thicker walled glass, C_2 and C_1 become more comparable even with very heavy elastomer coatings. In fact, for glass with d_o/d_i more than 2–3 at the tip it is probably not possible to achieve $C_2 < C_1$ in the tip region. Thus there are restrictions to the ratio of C_1 to C_2 that depend on the d_o/d_i ratio of the glass tubing, the geometry of the pipette, and the method elastomer coating. In fact, use of Eq. (8) for the entire immersed portion of the pipette is generally not appropriate if the d_o/d_i ratio of the glass and/or elastomer is not uniform. Instead, more accurate predictions can be made considering "sections" of the immersed portion of the pipette that are sufficiently short that the d_o/d_i ratio of the glass and elastomer can be considered to be constant in each section. Equation (8) can then be applied to each section and the results added together rms. Nevertheless, the equation with reasonable values of C_1 and C_2 for the entire immersed region can still be used to give good estimates of the amount of noise expected.

Equation (8) generally indicates that for any glass when the elastomer coating is thin the dielectric noise will depend primarily on the characteristics of the glass, whereas when the elastomer coating is very thick dielectric noise will become more dependent on the characteristics of the elastomer. However, the restrictions on the relative values of C_1 and C_2 must be borne in mind (and see later discussion of measured results). We begin by considering the situation for glasses other than quartz. The best glasses other than quartz that are presently readily available have dissipation factors in the range of 0.0022–0.005. These values are comparable to (or only somewhat higher than) the dissipation factor of Sylgard. Clearly, if $D_1 \approx D_2$ then Eq. (8) can be approximated by $[4kTc_2\pi B^2 D C_1 C_2/(C_1 + C_2)]^{1/2}$, where $D = D_1 = D_2$. This is simply the expected expression for two capacitors in series with identical dissipation factors. Thus, for example, if $C_2 = C_1$, then the overall pipette capacitance will be halved and the rms dielectric noise of the pipette will be reduced by 0.707×. In fact, since the dissipation factor of the glasses other than quartz is somewhat worse than that of Sylgard 184, the anticipated improvement will be somewhat greater in terms of dielectric noise.

For quartz the situation is different. If an uncoated quartz pipette has an immersion capacitance, C_1, of 1 pF and a dissipation factor of 0.0001, then from Eq. (7) it is predicted that its dielectric noise would be ~13-fA rms in a 5-kHz bandwidth (eight-pole Bessel filter). Coating with an elastomer with $D_2 = 0.002$ will generally *increase* the dielectric noise of such a pipette. For example, with a light coat of Sylgard 184 with a value of C_2 of 3 pF, dielectric noise calculated from Eq. (8) is predicted to be nearly 27-fA rms in the same bandwidth. With C_2 decreased to 1 pF (i.e., a thicker coat of elastomer), dielectric noise actually increases slightly more to ~29-fA rms in a 5-kHz bandwidth. Finally, with a very heavy coat of Sylgard bringing C_2 down to 0.3 pF it is predicted that dielectric noise will fall somewhat to about 24-fA rms in this bandwidth. Of course, this is still higher than the predicted value for the uncoated quartz pipette, but it must be remembered that without an elastomer coating thin-film noise will be present and that this will almost certainly be far worse than the small penalty in terms of dielectric noise (in addition the elastomer coating reduces distributed *RC* noise; see later discussion). Note that by the time C_2 has been reduced to 0.3 pF (30% of C_1), the predicted dielectric noise depends more on the characteristics of the elastomer than on that of the quartz. Thus, a pipette with an immersion capacitance of 0.3 pF and a dissipation factor of 0.002 (i.e., the characteristics of the elastomer coating) is predicted from Eq. (7) to have dielectric noise of about 31-fA rms, which is not much more than the predicted performance of the coated quartz pipette. Note that if an elastomer with a dissipation factor significantly less than that of Sylgard 184 can be found, then it can improve the performance of quartz pipettes (and, of course, pipettes fabricated from other glasses) even if its dissipation factor is still more than that of quartz (see Levis and Rae[8]). On paper, Dow Corning R-6101 might be such an elastomer since it is claimed by the manufacturer to have a dissipation factor of 0.00025. We believe this elastomer has some advantages, but to date significant improvements in noise has not been one of them. Tests indicate that it performs at least as well as Sylgard 184 in terms of noise reduction, but not significantly better in most situations. Note, however, that R-6101 tends to form thinner coats than does Sylgard 184; this is particularly true in the first millimeter behind the tip. This may be due to the longer time needed to cure R-6101, and may also have reduced the effectiveness of this coating in most of our tests to date.

Before leaving the subject of dielectric noise, it is important to note that the theory just presented has not always been entirely successful in predicting dielectric noise of all pipettes. As already described, we[8] found good agreement between actual measurements and the theoretical predictions of Eq. (8) for Sylgard 184 coated quartz pipettes (~35-fA rms in a

5-kHz bandwidth for a 1.8-mm depth of immersion). In that paper we also reported that similar pipettes fabricated from Corning 7052 and 7760 could display dielectric noise as low as ~70-fA rms (with somewhat higher values being more typical). This is more than would be predicted from Eq. (8). Similarly, Benndorf[10] found that actual measured dielectric noise (fitted f noise component attributable to pipette immersion) considerably exceeded theoretical predictions for pipettes fabricated from Schott 8330 (Duran). These pipettes differed very significantly in geometry from those we have used in most of our measurements, having very thick walls and small rapier-like tips. Nevertheless, the important point here is the discrepancy between theory and measurement. From the data of Benndorf[10] it can be calculated that for fits to actual measurements of the noise of a Sylgard coated pipette made from $d_o/d_i = 4$ Schott 8330 tubing with an immersion depth of 1 mm the f noise component (presumably dielectric noise of the pipette) attributable to immersion produced nearly 90-fA rms of noise in a 5-kHz bandwidth (eight-pole Bessel filter). This is roughly three times more than the theoretical prediction for an *uncoated* pipette with the same d_o/d_i ratio and same depth of immersion as judged from Ref. 10. The conclusion seems clear enough in terms of actual measured performance, a heavily Sylgard coated quartz pipette with an initial d_o/d_i ratio of 2.0 prior to pulling (1.4–1.5 near the tip after pulling) and an immersion depth of 1.8 mm produced measured dielectric noise (f noise) that is only somewhat more than one-third of the dielectric noise produced by a Sylgard coated borosilicate pipette with $d_o/d_i = 4$ prior to pulling (and apparently about 3.85 at the tip after pulling) with an immersion depth of only 1 mm. These results, coupled with our own measurements, seem to indicate clearly that quartz pipettes are significantly better in terms of dielectric noise reduction than pipettes fabricated from other glasses regardless of the elastomer coating. We cannot currently explain the difference between theoretical predictions and measured results of pipettes made from glasses other than quartz. In pipettes made from borosilicates of the geometry that we have used most frequently (and coated with Sylgard) the discrepancy is not quite as large as that just described from Benndorf.[10]

Root mean square dielectric noise in any particular bandwidth is expected to vary approximately with immersion depth, d, as $d^{1/2}$. This relationship would be precise if the d_o/d_i ratios of the glass and elastomer coating were constant over all of the immersed regions considered. This is because rms dielectric noise varies as the square root of capacitance. The nonuniformities already discussed (and see later discussion) will make the actual variation with immersion depth depart from this expectation to some extent. However, estimates based on detailed models of quartz pipettes with moderate to heavy Sylgard coating (with d_o/d_i ratios based on actual measure-

ments under a microscope) indicate that dielectric noise should not depart by more than about ±10% from the $d^{1/2}$ prediction.

DISTRIBUTED RC NOISE. Distributed *RC* noise arises from the distributed capacitance of the immersed portion of the pipette and the distributed resistance of its filling solution. The capacitance of the pipette is distributed reasonably evenly over the immersed portion. This statement must be qualified by the comments already made concerning likely thinning of the pipette wall near its tip and nonuniformities in the thickness of the elastomer coating. On the other hand, the resistance of the pipette is certainly very nonuniform. Most of the pipette resistance resides in regions near the tip. However, there is still considerable resistance in the regions distal to the tip. All of the pipette resistance produces thermal voltage noise, and this noise in series with the capacitance of the pipette produces current noise with a power spectral density that rises as f^2 over the range of frequencies important to patch clamping.

Figure 1B shows a very much oversimplified equivalent circuit representing distributed *RC* noise. This figure approximates the distributed situation with only four resistors (and their associated thermal voltage noise, not shown) in series with four capacitive elements, each made up of the capacitance of a section of the pipette wall and of the overlying elastomer. Obviously a more accurate distributed circuit would have many more resistive and capacitive elements. In any such circuit the first resistor (uppermost resistor in Fig. 1B) would represent all of the resistance of the portion of the pipette not immersed in the bath. The other resistors and capacitors would represent segments of the immersed portion of the pipette. In theoretical estimates of distributed *RC* noise, we have used such an equivalent circuit with many segments. (As many as 20,000 segments have been tested, but results that have converged to within about 10% can often be obtained with as few as ~30 *RC* segments.) However, such estimates may be crude because in order to make them accurate the values of the various elements must be known and this generally requires some sort of model of the pipette geometry that is likely to be oversimplified. We consider more realistic pipette models later, but we begin with some very simplified models of pipette geometry because these can form the basis for a more intuitive understanding of distributed *RC* noise. As an example of such a simple model, consider a pipette in which the tip and much of the shank are modeled as being of conical shape with a cone angle of 5.7 deg. If the electrode is filled with a solution with a resistivity of 50 Ωcm and has a tip diameter of 1 μm, then the expected resistance of the pipette is about 6.4 MΩ. Note that for simplicity it is assumed that this conical shape continues to a distance 5 mm back from the tip and that the electrode presents no further resistance beyond this point (e.g., the Ag|AgCl wire extends at

least this far into the pipette and effectively shunts any additional resistance). Such an electrode would have an internal diameter of 100 μm at a distance 1 mm back from the tip, 200 μm at a distance 2 mm from the tip, increasing to 500 μm at a distance of 5 mm. It is simple to calculate the resistance of sections of such a pipette due to its idealized geometry. Thus approximately 3.2 MΩ (half of the total resistance) resides within the first 10 μm from the tip. Another 2.13 MΩ resides in the region from 10 to 50 μm from the tip, and about 480 kΩ occurs in the next 50 μm (i.e., from 50 to 100 μm). In the region from 100 to 200 μm the additional resistance is about 280 kΩ; 180 kΩ occurs in the region from 200 to 500 μm; an additional 62 kΩ occurs from 500 to 1000 μm. Clearly resistance per unit length continues to decrease at distances further and further from the tip, however, another 51 kΩ occurs in the region from 1 to 5 mm beyond the tip. To estimate distributed *RC* noise for this simplified pipette it is also necessary to estimate the capacitance of the immersed portion of the pipette. Here we assume that the capacitance per unit length is constant (even though this is clearly an oversimplification as already described). Table II summarizes predicted results for different immersion depths and two different capacitances per mm of immersion. These are 1 pF/mm of immersion (corresponding roughly to a value of d_o/d_i of 1.25 for a dielectric constant of 4) and 0.25 pF/mm of immersion (corresponding to $d_o/d_i \approx 2.5$). All values are rms distributed RC noise for a bandwidth of 5 kHz (eight-pole Bessel filter). Noise for different bandwidths can be easily calculated by remembering that distributed *RC* noise will vary as $B^{3/2}$ (e.g., for a 10-kHz

TABLE II
PREDICTED DISTRIBUTED RC NOISE IN A 5 kHz BANDWIDTH[a]

Depth of immersion	1.0 pF/mm	0.25 pF/mm	Resistance of pipette not in bath (kΩ)
50 μm	15-fA rms	4-fA rms	1050
100 μm	23-fA rms	6-fA rms	569
200 μm	34-fA rms	8.5-fA rms	292
500 μm	54-fA rms	13.5-fA rms	113
1.0 mm	76-fA rms	19-fA rms	51
2.0 mm	102-fA rms	25.5-fA rms	19
3.0 mm	118-fA rms	29.5-fA rms	8.5

[a] The pipette geometry is assumed to be a simple cone with an angle of 5.7 deg and a constant d_o/d_i ratio producing an immersion capacitance of 1 or 0.25 pF/mm. A bandwidth of 5 kHz (−3 dB, eight-pole Bessel filter) is assumed. See text for further details.

bandwidth multiply all values by a factor of 2.83). For each depth of immersion the table also lists the amount of resistance for the portion of the pipette *not* immersed in the bath.

As expected the values of distributed *RC* noise fall by a factor of 4 for the 4-fold reduction in capacitance (all else being equal, rms values of distributed *RC* noise varies linearly with capacitance and as $R^{1/2}$ with resistance, R, provided that the resistance and capacitance change is uniform throughout the pipette—changes in pipette resistance due to tip diameter only have relatively little effect on distributed *RC* noise; see later discussion). Note that the reduction in capacitance can be brought about by either thicker walled glass tubing or heavy elastomer coating (but note that for these predictions to remain valid the geometry of the pipette lumen must be unchanged). Distributed *RC* noise does not depend on the type of glass used, except for the small dependence on dielectric constant. Note also that there is a large variation of distributed *RC* noise with depth of immersion. In fact, for this particular geometry the rms noise varies roughly as the square root of the depth of immersion (the relationship is somewhat steeper for small depths of immersion below about 500 μm and somewhat more shallow for depths of immersion greater than about 1 mm). Finally it should be pointed out that the predicted noise values are quite sensitive to the resistance in the portion of the pipette *not* immersed in the bath when the depth of immersion is relatively deep. Thus if for whatever reason this resistance were increased by 50 kΩ (so that, for example, it became 58.5 kΩ for an immersion depth of 3 mm), the rms noise would increase by a factor of about 1.6 for an immersion depth of 3 mm (to nearly 200-fA rms for the 1 pF/mm pipette), by a factor of about 1.4 for a 2-mm depth of immersion, and by a factor of 1.2 for a 1-mm depth of immersion. However, for a 200-μm depth of immersion the noise would only increase by about 4%.

The results just described provide some insight into distributed RC noise and suggest obvious methods to minimize it. It is important to realize, however, that these results are highly dependent on the particular geometry chosen and therefore on the oversimplified model considered. Nevertheless, it is very clear that distributed *RC* noise can be minimized by using thick-walled pipettes (glass plus elastomer) and shallow depths of immersion. Because coating the tip region of the pipette with thick layers of elastomer is very difficult, thick-walled glass, pulled so as to preserve the d_o/d_i ratio as much as possible, is probably the most convenient and practical method of reducing the capacitance of the immersed portion of the pipette near the tip. Heavy elastomer coating can further reduce pipette capacitance even when thick-walled glass is used. Shallow depths of immersion can also be important to minimizing distributed RC noise, but this may not always

be possible, and besides the precise depth of immersion can be affected by a meniscus of solution as the pipette emerges from the bath (see also predictions for more realistic elastomer coating below).

Because of uncertainties involved in theoretical estimates of distributed *RC* noise, Levis and Rae[8] attempted to measure this noise directly. These measurements relied on the fact that changing the ionic strength of the filling solution would affect the pipette resistance but not its capacitance. Thus noise was measured for pipettes coated with Sylgard only roughly above the point where the pipette entered the bath (to maximize distributed *RC* noise, in these studies this was about 2 mm back from the tip) with ionic filling solutions varying from 5 m*M* to 1.5 *M*. Quartz pipettes with an initial (prior to pulling) d_o/d_i ratio of 2.0 were used in these investigations and the pipettes were sealed to Sylgard at an immersion depth of about 1.8 mm. It was concluded that the distributed *RC* noise for the pipette geometry used had a PSD of about $2.5 \times 10^{-38} f^2$ amp^2/Hz for 150 m*M* NaCl filling solution. This would indicate an rms noise of $(8.3 \times 10^{-39} c_3 B^3)^{1/2}$ where c_3 is as usual a coefficient that depends on the type of filter used ($c_3 \approx 2$ for an eight-pole Bessel filter). This indicates an rms noise of about 45-fA rms in a 5-kHz bandwidth. Of course, estimating distributed *RC* noise required that other sources of noise be estimated and subtracted from the measurement; we relied heavily on the fact that in this situation the major source of f^2 noise associated with immersion of the pipette should be distributed *RC* noise. The need to separate noise components introduces some uncertainty into the estimate of each component. These results were in reasonable agreement with (or slightly less than) expectations based on theoretical predictions for the pipette geometry used in these studies. More precise simulations of distributed *RC* noise for pipettes of geometry similar to those used by Levis and Rae[8] are considered later. First, however, a few more simulations of simplified geometries are considered.

It is important to realize that pipette geometry involved in determining pipette resistance can have very significant effects on distributed *RC* noise even if the d_o/d_i ratio of the pipette (glass plus elastomer) is kept constant. This can be appreciated by comparing idealized geometries of the type already described with different cone angles. For this purpose we consider cone angles of 12, 6, 3 and 1.5 deg. In all cases the tip diameter is assumed to be 0.5 μm (note that tip diameter per se has relatively little effect on distributed *RC* noise in these models; see later discussion). The capacitance of the pipette was assumed to be 0.5 pF/mm of immersion (a constant d_o/d_i ratio has been assumed over the immersed region). Table III reports predicted rms distributed *RC* noise in a 5-kHz bandwidth (eight-pole Bessel filter) for each of the pipette geometries. Once again it is assumed

TABLE III
PREDICTED DISTRIBUTED RC NOISE FOR PIPETTES WITH DIFFERENT CONE ANGLES[a]

Depth of immersion	Cone angle			
	12°	6°	3°	1.5°
50 μm	4.0-fA rms	7.8-fA rms	14-fA rms	25-fA rms
100 μm	5.8-fA rms	11.3-fA rms	22-fA rms	40-fA rms
200 μm	8.4-fA rms	16.5-fA rms	32-fA rms	60-fA rms
500 μm	13-fA rms	26-fA rms	52-fA rms	100-fA rms
1.0 mm	18-fA rms	37-fA rms	72-fA rms	145-fA rms
2.0 mm	25-fA rms	49-fA rms	97-fA rms	192-fA rms
3.0 mm	28-fA rms	56-fA rms	112-fA rms	222-fA rms

[a] A bandwidth of 5 kHz (−3 dB, eight-pole Bessel filter) is assumed for all values listed. Cone angles are assumed to be constant over the relevant portion of the pipette, and the capacitance of the pipette is assumed to be 0.5 pF/mm of immersion. Tip diameter is 0.5 μm. See text for further details.

that there is no further resistance after a distance 5 mm back from the tip.

Large cone angles can clearly be useful in minimizing distributed *RC* noise, but may not always be compatible with other requirements. For example, in our experience large cone angles (e.g., 12 deg) are difficult to achieve over extended regions of the pipette with thick-walled glass. Note that for filling solutions with a resistivity of 50 Ωcm the resistance of these electrodes would be about 6, 12, 24, and 49 MΩ for cone angles of 12, 6, 3, and 1.5 deg, respectively. Had the tip diameter been increased to 1 μm these resistances would have been cut in half, however, the distributed RC noise in no case would have decreased by more than about 6%. The largest decreases (i.e., ~6%) would occur for very shallow depths of immersion; for immersion depths of 1 mm or more the reduction would be less than 2%. Increasing the tip diameter to 2 μm (which would drop the total electrode resistance to only about 25% of the values listed above) would have decreased distributed *RC* noise by less than 15% in all cases, and for depths of immersion of 1 mm or more the decrease is considerably less. Decreasing the tip diameter below 0.5 μm similarly only produces relatively small increases in distributed RC noise. Thus it is very important to note that electrode resistance by itself is not a reliable indicator of anticipated distributed RC noise. Instead it is the overall geometry of the electrode that must be considered. The reason that tip diameter has such a small effect on distributed *RC* noise is that despite the fact that most of the resistance of the pipette resides very close to the tip, very little of the pipette immersion capacitance is in this region. The *relative* amount of capacitance near the

tip is greater when the immersion depth is small than when the pipette is deeply immersed in the bath. This accounts for the larger effects of tip diameter on distributed RC noise with shallow depths of immersion.

Once again it must be emphasized that the geometries just considered are highly oversimplified, so that the values listed in Table III should only be thought of as guidelines for the amount of variation of distributed *RC* noise that is possible with different geometries. Remember also that these values have assumed a particular capacitance per millimeter of immersion (0.5 pF in this case) and that rms distributed *RC* noise will scale linearly with this capacitance. Moreover, it has been assumed that the capacitance per unit length is constant. This assumption may not be unreasonable relatively near the tip where building up a heavy elastomer coat is difficult, but remember that at distances about 0.5–1 mm from the tip building up heavy coats of elastomer is quite easy and this will reduce the capacitance per unit length in these regions. It is also clear that the assumption of a single cone angle from the tip back to a distance 5 mm behind the tip is not realistic, particularly for the smallest cone angles (e.g., for the 1.5-deg cone angle this means an inner diameter of only 131 μm at a distance of 5 mm from the tip). In addition, the assumption that there is no resistance beyond 5 mm from the tip is clearly an oversimplification. In some pipette geometries the internal diameter has almost reached the original inner diameter of the tubing by a distance of as little as 3 mm, and it would be better to assume no significant resistance sooner; in other pipettes there may still be significant resistance even further back from 5 mm from the tip. Thus the numbers in Table III are not meant to be representative of real pipettes. Instead, they are intended to show the large variations of distributed *RC* noise that are possible with differing pipette geometries.

Benndorf[10] has recently investigated distributed RC noise for pipettes with very shallow cone angles (at least for the first 200 μm from the tip), thick walls (d_o/d_i as much as 8), and very small tip openings (~0.2 μm). These pipettes generally had resistances of 50–90 MΩ when filled with 200% Tyrode solution (specific resistance $\approx$ 26 Ωcm). The pipettes were fabricated from Duran (Schott 8330). This geometry of pipette was used for a variety of reasons, including (1) very high seal resistances (up to 4000 GΩ) were obtained with very small tipped pipettes and (2) the slender pipette geometry near the tip is very effective in preserving the d_o/d_i ratio during pulling. Benndorf measured the resistance of a "prototype pipette" over the first 200 μm behind the tip and used these data (presumably plus a largely unspecified model of the rest of the pipette) to calculate distributed *RC* noise. This pipette (which was typical of those used in that study) had a very shallow cone angle which, over the range from ~80 to 200 μm, can be estimated to be roughly 0.6 deg, but increases somewhat nearer the tip.

No data are presented concerning the electrode geometry further than 200 μm from the tip, except that it is noted that the fitted value of the resistance after breaking the pipette off 200 μm from the tip ("R_{200}") was 2 MΩ.[18] A number of theoretical calculations of distributed RC noise are presented for different d_o/d_i ratios and immersion depths ranging from ~10 μm to 1 mm. Unfortunately the details of these calculations—particularly in terms of assumed pipette geometry at distances greater than 200 μm form the tip—are not presented. Both uncoated and Sylgard coated pipettes were considered and the assumption was made that the d_o/d_i ratio was constant in both cases. It was concluded that distributed *RC* noise increases rapidly with immersion depth up to a depth of about 200 μm, but that further immersion had relatively little effect on predicted distributed *RC* noise. Indeed, for immersion depths greater than 300–400 μm there seems to be essentially no increase in predicted distributed *RC* noise with further immersion of the pipette. This behavior is quite different than the theoretical predictions we described earlier (see Tables II and III). Considering Table II it can be seen from the tabulated data that the predictions of the simple model considered suggest that distributed *RC* noise continues to increase significantly as immersion depth increases. Clearly the slope of the variation of distributed *RC* noise with immersion depth decreases with increasing depth of immersion, but, for example, increasing immersion depth from 200 μm to 1 mm increases the predicted distributed *RC* noise by a factor of somewhat more than 2. However, as already noted the assumptions of a constant cone angle and particularly of a constant capacitance per millimeter of immersion are not realistic (although the latter assumption was also made by Benndorf[10]).

To clarify the expected noise, we studied the geometry of a typical pipette of the type we most often use in greater detail. This pipette was fabricated from $d_o/d_i = 2.0$ quartz tubing and pulled on the Sutter P-2000. Its tip diameter was approximately 0.5 μm. We carefully measured the inner and outer diameter at various distances from the tip. We found that the interior of the pipette could be very reasonably approximated out to a distance of about 3 mm from the tip by three different cones. The first cone going from the tip to a distance 100 μm behind the tip had an angle of ~6.6 deg (bringing the inner diameter to about 12 μm at 100 μm from the tip). The second cone extended from 100 to 600 μm from the tip and

[18] This value is somewhat surprising, since if the same cone angle continued from 200 to 300 μm from the tip this region alone would add approximately 5 MΩ to the total resistance of the pipette. To achieve a value of R_{200} of only 2 MΩ, the cone angle would have to increase dramatically after 200 μm, although there is no indication of the beginnings of such an increase in the data shown.

had a more shallow angle of only ~2.7 deg (bringing the inner diameter to about 36 μm at a distance of 600 μm from the tip). The third cone extends from 600 μm to about 3 mm and had an angle of 6.1 deg (bringing the inner diameter to somewhat more than 290 μm at a distance of 3 mm from the tip). Beyond 3 mm, the inner diameter quickly increased toward that of the original tubing (750 μm) so that it was within roughly 10% of this diameter at 5 mm from the tip. At all distances from the tip out to 3 mm from the tip this relatively simple model gave inner diameters that agreed with actual measurements of the pipette to better than ±5%. Several other pipettes pulled with the same settings were also examined and found to be very similar to that just described. The outer diameter of the pipette was modeled as having a d_o/d_i ratio of 1.5 in the first cone, 1.55 in the second cone, and 1.6 in the third cone. This produced reasonable agreement with measured ratios, but not as precise as the agreement between model and measured inner diameters. In particular, it was found in some pipettes that the thinning of the pipette wall during pulling could be greater on one side of the pipette than on the other. This is presumably due to the characteristics of the laser puller, but was not taken into account in this model.

The Sylgard coat was applied by the dip method described by Levis and Rae.[8] Only a single dip was used for the data to be considered at this point, although prior to this dip a ring of Sylgard was painted and cured about 2 mm back from the tip. The thickness of this coating was then carefully measured under the microscope at various distances from the tip. It was found that at the tip in this situation the d_o/d_i ratio of the Sylgard coat (i.e., the outer diameter of the coated pipette divided by the outer diameter of the glass) was only about 1.1, while at 2–3 mm from the tip this ratio can be 4 or more. The approximate d_o/d_i ratios of the Sylgard coat at various distances from the tip were as follows:

Distance from tip (μm)	d_o/d_i Ratio of Sylgard
50	1.12
100	1.16
200	1.2
300	1.35
500	1.6
1000	2.2
2000	3.4
3000	4.6

The form of the model pipette with its Sylgard coating is shown in Fig. 2. Note that Fig. 2 shows the diameter of the inner and outer walls of the

quartz and the outer edge of the Sylgard coating as a function of distance from the tip, but the radial and longitudinal scales are different. Figure 2A shows the model for the first 3 mm beyond the tip and Fig. 2B shows an expanded view of the first 1 mm. While the wall of the quartz pipette model has a reasonably constant d_o/d_i ratio (somewhat more so than the actual pipette), the Sylgard coating can easily be seen to be extremely nonuniform.

This model was then used to compute distributed *RC* noise in an uncoated pipette and a pipette with a Sylgard 184 coating as shown in Fig. 2. The resistance was computed on the basis of the inner diameter of the model assuming that the specific resistance of the filling solution was 50 Ωcm. Computations were made using segment lengths of only 0.2 μm for up to 3 mm back from the tip (the largest depth of immersion considered). The resistance from 3 to 5 mm from the tip was estimated to be 4 kΩ, and it was assumed that there was no additional resistance beyond 5 mm from the tip. The total pipette resistance is estimated to be ~11.5 MΩ. The capacitance per unit length in the case of an uncoated pipette was somewhat different in each cone; namely, 0.52 pF/mm in the first cone, 0.48 pF/mm in the second cone, and 0.45 pF/mm in the third cone. In the case of the Sylgard coated pipette, the capacitance per unit length was set in 13 different regions giving a good approximation to the measured data. These regions were of shorter length near the tip and increased in length at greater distances from the tip. The average d_o/d_i ratio of the Sylgard coating in each region was approximated and this information combined with the d_o/d_i ratio of the quartz pipette of the model was used to determine the capacitance per unit length in each region. This varied from about 0.39 pF/mm at the tip to as little as 0.09 pF/mm at 2.6 to 3 mm from the tip.

The results of these simulations are summarized in Fig. 3 for immersion depths up to 3 mm; the bandwidth considered is 5 kHz (eight-pole Bessel filter), but recall that any other bandwidth can be determined by remembering that distributed *RC* noise varies as $B^{3/2}$. Upper curve (a) in Fig. 3 shows the prediction for the uncoated pipette and lower curve (b) shows the prediction for the Sylgard-coated pipette. It is worthwhile to compare these results to the measured data from Levis and Rae[8] at an immersion depth of 1.8 mm (the depth used in that study). At this depth the uncoated pipette is predicted to have distributed *RC* noise of about 55-fA rms and a current noise PSD of $3.6 \times 10^{-38} f^2$ amp^2/Hz. This is about 40% higher than the estimated PSD of $2.5 \times 10^{-38} f^2$ amp^2/Hz reported by Levis and Rae,[8] and the rms noise predicted by the simulation is about 20% higher than the 45-fA rms estimated in that study for the same bandwidth and depth of immersion. However, the agreement seems reasonable considering likely differences in the geometry of the pipettes in the two cases (the pipettes used here were similar to—but certainly not identical to—those used in

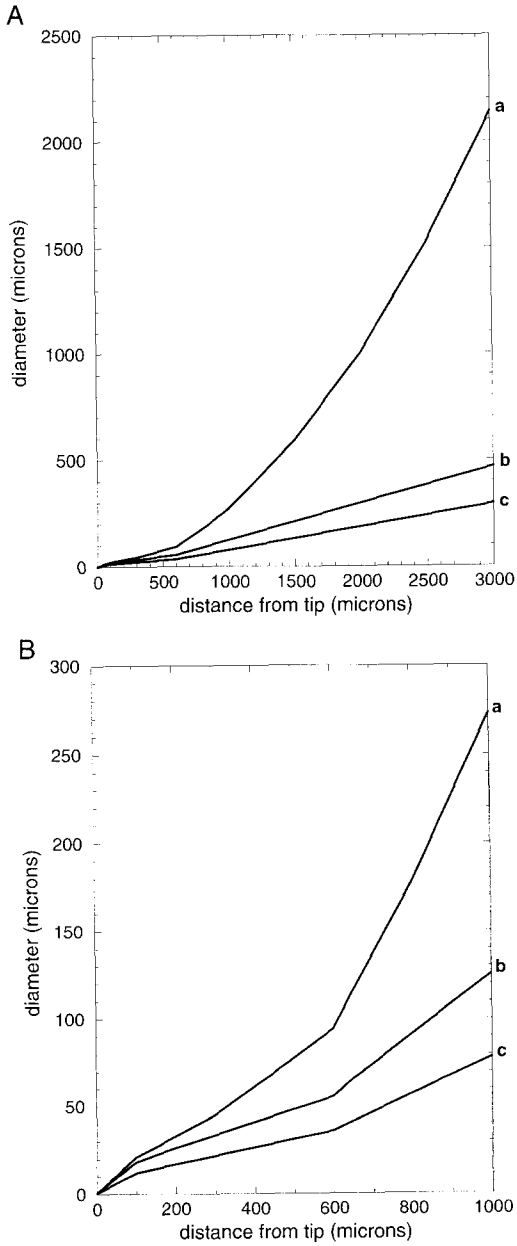

FIG. 2. Geometry of the pipette model used to compute distributed *RC* noise shown in Fig. 3. Note the plots of the diameter (not radius) of the pipette (inner and outer diameter) and of the elastomer coating (outer diameter). The geometry of the pipette and its elastomer coating is based on detailed microscopic measurements of an actual pipette pulled from d_o/

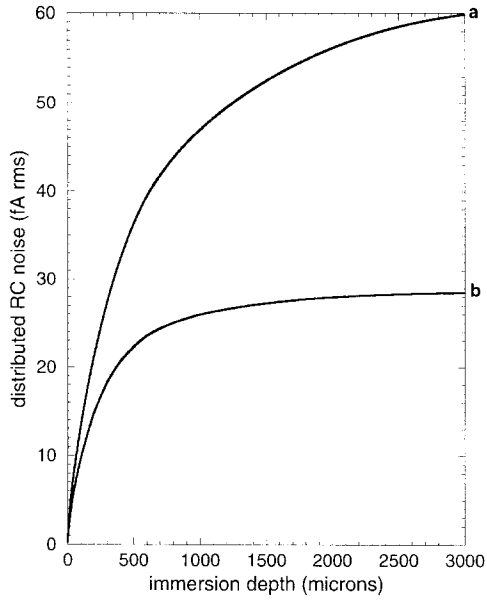

FIG. 3. Predictions of rms distributed *RC* noise as a function of immersion depth for a bandwidth of 5 kHz (−3 dB, eight-pole Bessel filter) for a pipette with the geometry illustrated in Fig. 2. The pipette is assumed to be fabricated from quartz (dielectric constant of 3.8) and the elastomer coating is Sylgard 184 (dielectric constant of 2.9). Since the dielectric constant of borosilicate glasses is only about 20–30% higher than that of quartz, predictions for such glasses pulled to the same geometry would only be somewhat higher. Curve (a) is predicted rms distributed *RC* noise for an *uncoated* pipette of the geometry shown in Fig. 2 and curve (b) is predicted rms distributed *RC* noise for the same pipette with a coating of Sylgard 184 as illustrated in Fig. 2. See text for further details.

the previous study). However, in the previous study we predicted that the PSD of distributed *RC* noise of the pipette would vary as C_c^2, where C_c is the capacitance of the immersed portion of the pipette, including both the glass and the elastomer; specifically we suggested that for the pipettes used at the time the PSD of distributed *RC* noise might be estimated by $\sim 10^{-14} C_c^2 f^2$ amp^2/Hz. For a 2-mm depth of immersion the model pipette with its Sylgard coating has a capacitance, C_c, of about 0.35 pF. Based on

---

d_i = 2 quartz tubing. (A) First 3 mm of the pipette and its elastomer coating. (B) Expanded view of the first 1 mm of the model pipette. In both parts (A) and (B) curve (a) is the outer diameter of the Sylgard coat, (b) is the outer diameter of the quartz pipette, and (c) is the inner diameter of the pipette. See text for further details. [Reprinted from R. A. Levis and J. L. Rae, The use of quartz pipettes for low noise single channel recording. *Biophys. J.* **65**, 1666–1667 (1993).]

our previous suggestion, this would produce an estimated PSD of about $1.2 \times 10^{-39} f^2$ amp^2/Hz at this depth of immersion and thus predicts about 10-fA rms of noise in a 5-kHz bandwidth. However, the present simulation indicates a PSD of about $9 \times 10^{-39} f^2$ amp^2/Hz for this depth of immersion and predicts about 28-fA rms in a 5-kHz bandwidth. The reason for this discrepancy is simple: in forming our earlier prediction we[8] made the assumption of a uniform d_o/d_i ratio, and thereby failed to take into account the extreme nonuniformity of the coating of Sylgard. The Sylgard coating is quite thin near the tip of the pipette and only becomes comparable to or greater than the quartz pipette wall in terms of d_o/d_i ratio at distances of 500 μm from the tip. Because of this most of the distributed *RC* noise in the elastomer-coated pipette arises relatively near the tip and it significantly exceeds the previous predictions for a Sylgard-coated pipette of roughly this geometry.

Examination of the two curves in Fig. 3 shows that for the uncoated pipette there is a significant variation of distributed *RC* noise with immersion depth all the way to 3 mm. In fact, the form of the curve is quite similar to that produced by the simpler model used for computing Table II. On the other hand, the Sylgard-coated pipette shows relatively little increase in distributed *RC* noise at immersion depths beyond about 1 mm. The reason for this (as just explained) is that the Sylgard coating is very thin near the tip but becomes quite thick at distances beyond 0.5–1 mm from the tip. The reduced variation of distributed *RC* noise with immersion depths greater than ~1 mm in the model pipette with Sylgard coating is somewhat reminiscent of the theoretical calculations presented by Benndorf.[10] However, note that Benndorf's predictions show even less variation at distances beyond 200 μm from the tip, and that this low variation cannot be accounted for by the nonuniformity of an elastomer coat. Benndorf[10] assumed that the d_o/d_i ratios in his pipette models were completely constant with and without elastomer coatings.

We have also investigated methods of building up heavier coats of elastomer and pipettes pulled from $d_o/d_i = 4$ quartz tubing. Our investigations of very thick-walled quartz pipettes have to date been rather limited, but with settings that are essentially the same as those used to pull the pipette approximated in Fig. 2, we achieve a pipette with a d_o/d_i ratio that varies from about 2.5 to 3.5 over the first 3 mm from the tip. The area within 100 μm of the tip actually has a slightly higher d_o/d_i ratio than somewhat more distal regions, but we feel that approximating the d_o/d_i ratio as 2.7 is reasonable for the entire first 3 mm. Based on measurements of the actual pipette we concluded that the interior of the pipette could be modeled quite reasonably over the first 3 mm as three conical sections. The first cone had an angle of 2 deg and extended from the tip to 350 μm; the

second cone extended from 350 μm to 1 mm and had an angle of 4.2 deg; the third cone extended from 1 to 3 mm and had an angle of only 1.4 deg. The geometry of this pipette model is shown in Fig. 4. (Figure 4 also shows a very heavy Sylgard layer described below.) Just prior to 3 mm from the tip the inner diameter of the actual pipette began to increase rapidly, reaching about 90% of the initial inner diameter of the tubing (375 μm) by 5 mm back from the tip. The tip diameter was taken to be 0.5 μm and the resistance of the pipette filling solution (specific resistance = 50 Ωcm) from 3 to 5 mm was taken to be 12 kΩ, and, as before, it was assumed that there was no further resistance beyond 5 mm from the tip. The total predicted resistance of the pipette is about 35 MΩ. Predictions of distributed *RC* noise (rms noise in a 5-kHz bandwidth established by an eight-pole Bessel filter) for an *uncoated* pipette with this geometry are shown as the uppermost curve (a) of Fig. 5. It can be seen by comparison with Fig. 3 that the predicted distributed *RC* noise in this case is only somewhat less than for the uncoated pipette pulled from $d_o/d_i = 2$ tubing. At an immersion depth of 1.8 mm the predicted noise of this pipette is about 44-fA rms. It can also be seen in this case that the dependence of distributed *RC* noise on immersion depth is greater for the thick-walled pipette. The reason that noise only decreased slightly despite a significant increase in the d_o/d_i ratio is the much smaller bore of the pipette, which has only reached an inner diameter of 109 μm at a distance of 3 mm back from the tip; this also explains the steeper dependence of the noise on immersion depth. Thus, an increased d_o/d_i ratio by itself may not be very useful in reducing distributed *RC* noise—the geometry of the pipette lumen must also be considered.

On the other hand, heavier elastomer coatings than those considered above can continue to reduce distributed *RC* noise significantly. We have used the following technique to build up heavier coats of Sylgard 184. Paint a relatively heavy blob of elastomer entirely around the shank of the pipette just below where the pipette begins to taper. Then place the tip of the painted pipette into the prewarmed blowing air from a heat gun with the tip *pointing at the ground* and twirl the pipette around its long axis until the elastomer is cured. This results in an elastomer with a large blunt front edge about halfway up the tapered region of the pipette. Repeat this entire procedure one or two more times, each time placing the elastomer blob just in front of (i.e., toward the tip) of the blunt end of the cured elastomer. Then, if desired, paint elastomer over the outside of all the existing elastomer simply to obtain a uniform thickness over the entire coated area. Finally, any uncoated area at the tip can be coated using our previously described[8] "tip dip" method. With practice, the entire process can be completed in about 3–4 min. This can produce quite striking results as illustrated in Fig. 4. This figure shows the inner and outer diameter of the model of

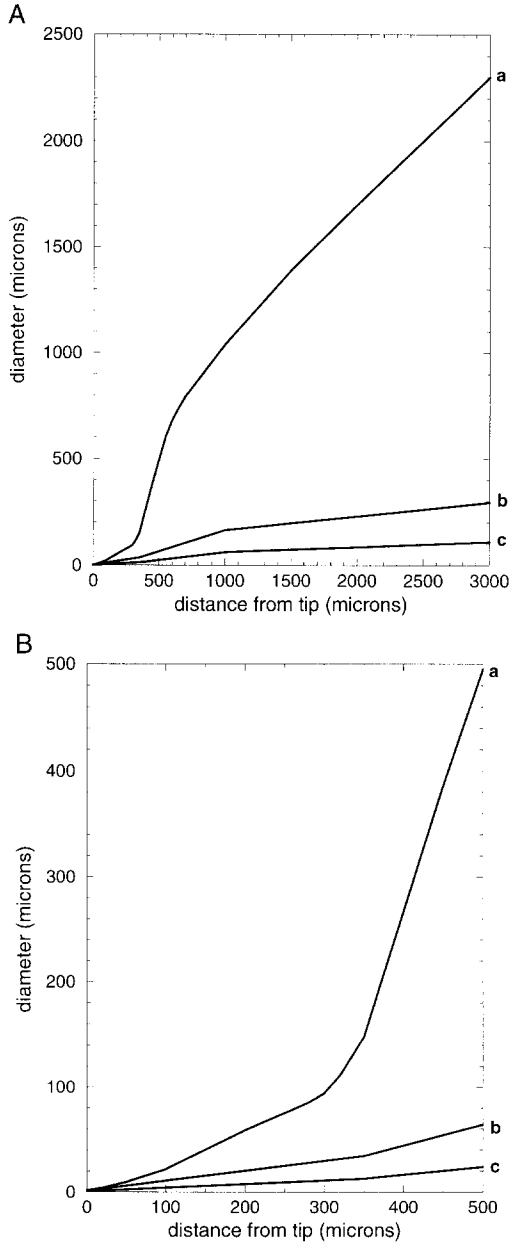

FIG. 4. Geometry of the pipette model used to compute distributed *RC* noise shown in Fig. 5. As in Fig. 2, this figure plots the diameter (not radius) of the pipette (inner and outer diameter) and of the elastomer coating (outer diameter). The geometry of the pipette and

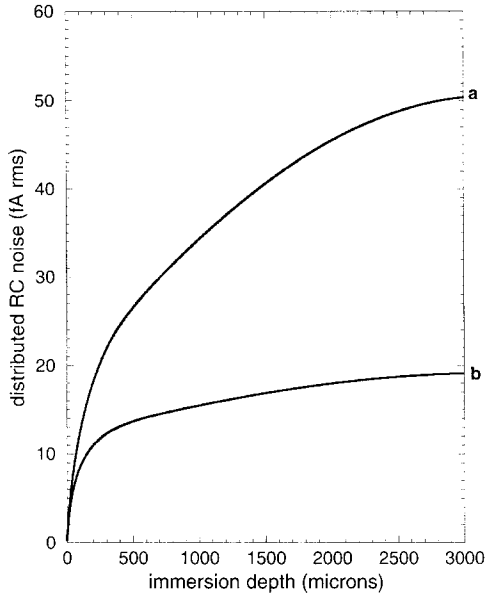

FIG. 5. Predictions of rms distributed *RC* noise as a function of immersion depth for a bandwidth of 5 kHz (−3 dB, eight-pole Bessel filter) for a pipette with the geometry illustrated in Fig. 4. As in Fig. 3, the pipette is assumed to be fabricated from quartz (dielectric constant of 3.8) and the elastomer coating is Sylgard 184 (dielectric constant of 2.9). Since the dielectric constant of borosilicate glasses is only about 20–30% higher than that of quartz, predictions for such glasses pulled to the same geometry would only be somewhat higher. Curve (a) is predicted rms distributed *RC* noise for an *uncoated* pipette of the geometry shown in Fig. 4 and curve (b) is predicted rms distributed *RC* noise for the same pipette with a coating of Sylgard 184 as illustrated in Fig. 4. Note that a Sylgard coat with the same d_o/d_i ratio as that considered here applied to a pipette with the geometry shown in Fig. 2 is predicted to produce somewhat *less* distributed RC noise than is shown in curve (b). However, the reduction is only 15%. See text for further details.

the pipette pulled from $d_o/d_i = 4$ quartz tubing described above and the outer diameter of a heavy layer of Sylgard as measured following application to such a pipette by the procedure just described. Figure 4A shows the first 3 mm of the pipette and Fig. 4B shows an expanded view of the first 500

its elastomer coating is based on detailed microscopic measurements of an actual pipette pulled from $d_o/d_i = 4$ quartz tubing. The heavy elastomer coat was produced by the method described in the text. (A) First 3 mm of the pipette and its elastomer coating. (B) Expanded view of the first 500 μm of the model pipette. In both parts (A) and (B) curve (a) is the outer diameter of the Sylgard coat, (b) is the outer diameter of the quartz pipette, and (c) is the inner diameter of the pipette. See text for further details.

μm. Although we have been unable to get the Sylgard coat to have a d_o/d_i ratio greater than about 1.1 at the tip itself, the d_o/d_i ratio has increased to more than 1.5 at a distance of 50 μm back from the tip and to 2.0 at 100 μm from the tip. The Sylgard layer increases dramatically after about 300 μm with d_o/d_i ratios over 5.0 occurring at distances beyond 500 μm from the tip. Thus, except very close to the tip, it is possible to produce very heavy elastomer coatings. Note that such heavily coated pipettes could be hard to work with, since the overall pipette diameter becomes quite large quite quickly. However, with a little practice the shape of the elastomer coating can be adjusted fairly easily. It is important to note that although the d_o/d_i ratio of the elastomer has been increased at all distances more than a few microns from the tip, this ratio remains extremely nonuniform.

Results of simulations of distributed *RC* noise for the pipette pulled from $d_o/d_i = 4$ quartz tubing and the Sylgard layer illustrated in Fig. 4 are also presented in Fig. 5, curve (b). Immersion depths up 3 mm are shown and, as in the uncoated curve, a 5-kHz bandwidth is assumed. It can easily be seen that distributed *RC* noise is greatly reduced by the heavy elastomer coating at all depths of immersion, with a predicted value of less than 18-fA rms at an immersion depth of 1.8 mm. However, to reach values less than 10-fA rms the depth of immersion would have to be less than 200 μm, and this is often impractical (probably particularly so with a pipette with so much elastomer coating). Different pipette geometries pulled from $d_o/d_i = 4$ tubing can yield somewhat better results, but the noise levels already described are probably small enough for even very demanding applications.

Finally, note that, as expected, a very heavy coat of Sylgard 184 similar in appearance (approximately the same d_o/d_i ratio for the elastomer coating) to that shown in Fig. 4 can further reduce the distributed *RC* noise of pipettes of geometries other than that shown in Fig. 4 for $d_o/d_i = 4$ quartz. For example, a simulation with the pipette geometry illustrated in Fig. 2 (i.e., a pipette pulled from $d_o/d_i = 2$ quartz tubing) with a heavy Sylgard coating with essentially the same d_o/d_i ratio of the elastomer coating shown in Fig. 4 actually produced slightly less distributed *RC* noise than that predicted for the pipette pulled from $d_o/d_i = 4$ quartz tubing. The predicted improvement (~15-fA rms for a 5-kHz bandwidth at an immersion depth of 1.8 mm) was not very large, although the variation of noise with immersion depth was also reduced. This indicates that for distributed *RC* noise both overall (glass plus elastomer) wall thickness and the geometry of the pipette lumen need to be considered. The $d_o/d_i = 2$ quartz tubing pulled to pipettes similar to that shown in Fig. 2 and heavily coated with elastomer is adequate in terms of distributed *RC*, although somewhat less dielectric noise is predicted for pipettes pulled from $d_o/d_i = 4$ quartz.

Our theoretical and experimental results suggest that for pipettes of the geometry we most commonly use pulled from tubing with $d_o/d_i = 0.2$ and with a moderate to heavy elastomer coating distributed *RC* noise can be kept to below 30-fA rms in a 5-kHz bandwidth for a depth of immersion of at least 2 mm. This figure can be roughly cut in half with extremely heavy Sylgard coatings such as those illustrated in Fig. 4. The expected noise depends only slightly (due to different dielectric constants) on the type of glass. With $d_o/d_i = 4.0$ tubing distributed *RC* noise may be reduced somewhat, although this depends on the geometry of the pipette and the degree of elastomer coating. Smaller depths of immersion can reduce distributed *RC* noise further.

It is worthwhile to compare the expected magnitudes of distributed *RC* noise and dielectric noise. While distributed *RC* noise does not depend significantly on the type of glass used, glass type seems to be even more important to dielectric noise than is theoretically predicted. With quartz pipettes (elastomer coated, initial d_o/d_i ratio = 2) at an immersion depth of about 2 mm measured dielectric noise is about 30- to 35-fA rms in a 5-kHz bandwidth. More precise calculations of dielectric noise for the model quartz pipettes shown in Figs. 2 and 4 using distributed models that take into account the nonuniformities in d_o/d_i ratio of the quartz and the Sylgard predict dielectric noise of ~27-fA rms and ~17-fA rms for the pipettes of Figs. 2 and 4, respectively, at a 2-mm depth of immersion. Dielectric noise in both cases varies roughly (but not precisely) as the square root of immersion depth. On the other hand, with borosilicate glasses, even with heavy elastomer coatings, measured dielectric noise is generally ≥70-fA rms in a 5-kHz bandwidth, which is significantly more than would be theoretically predicted. Thus, at this bandwidth and a 2-mm depth of immersion, dielectric noise is comparable to distributed *RC* noise for quartz and significantly higher than distributed *RC* noise for borosilicate pipettes of the geometries considered here. Fortunately, minimizing distributed *RC* noise and dielectric noise generally requires the same basic strategy, that is, use of thick-walled glass (tubing $d_o/d_i \geq 2$), heavy elastomer coating, and shallow depth of immersion. However, the degree to which each of these measures reduces distributed *RC* noise and dielectric noise is sometimes different. For example, geometry of the pipette lumen must be considered in the case of distributed *RC* noise, but is essentially unimportant to dielectric noise. Large cone angles can be useful in reducing distributed *RC* noise, but will not directly affect dielectric noise; moreover, large cone angles may not be practical or possible with thick-walled tubing, which is otherwise beneficial to the reduction of both distributed *RC* noise and dielectric noise. Nevertheless, the same basic strategy generally applies to minimizing both types of noise. However, there are two major distinctions between factors determin-

ing distributed RC noise and dielectric noise that must be remembered: (1) effects of glass type and (2) variation of noise with bandwidth. Glass type has already been considered in detail, but it is worth recalling that the use of quartz has been shown to be important to minimizing dielectric noise, but is largely unimportant to the reduction of distributed RC noise. The bandwidth of the measurement will affect the *relative* magnitudes of these noise types since rms dielectric noise increases with increasing bandwidth (B) linearly, while distributed RC noise increases as $B^{3/2}$. For each doubling of the bandwidth, dielectric noise increases by a factor of 2 while distributed RC noise increases by a factor of 2.83. Thus, as bandwidth increases the importance of distributed RC noise relative to dielectric noise increases.

R_e-C_p NOISE. R_e-C_p noise arises from the entire (lumped) resistance of the pipette, R_e, in series with the capacitance of the patch, C_p. Of course, in most single-channel measurement situations the capacitance of the patch is very small. Nevertheless, this small capacitance is in series with the thermal voltage noise of a large resistance and can therefore sometimes produce significant amounts of noise. Over the frequency range of interest to patch clamping the PSD of R_e-C_p noise, S_{ep}^2, rises with increasing frequency as f^2. This PSD is given by:

$$S_{ep}^2 = 4\pi^2 e_e^2 C_p^2 f^2 \qquad \text{amp}^2/\text{Hz} \tag{9}$$

where $e_e^2 = 4kTR_e$ is the thermal voltage noise PSD of the pipette resistance. This equation can be integrated over a bandwidth B (DC to B Hz) to give an expression for the rms noise, i_{ep}, attributable to this mechanism:

$$i_{ep} = \{(4/3)\pi^2 c_3 e_e^2 C_p^2 B^3\}^{1/2} \qquad \text{amp rms} \tag{10}$$

where c_3 is a coefficient that depends on the type of filter used as described previously, and R_e can range from as little as ~1 MΩ to many tens of megohms for typical patch-clamp measurements. For traditional patches C_p is expected to fall in the range of a few to perhaps 300 fF. Although the relationship is not perfect, it is expected that higher resistance pipettes with smaller tips will have smaller patches with less capacitance. It can be seen from Eq. (10) that the rms value of R_e-C_p noise depends linearly on C_p but on the square root of R_e. Thus this noise is minimized by small patches even if these are associated with high-resistance pipettes. An unfavorable example of R_e-C_p noise would be a 2-MΩ pipette with a 300-fF patch. From Eq. (10) it can easily be calculated that this would result in nearly 100-fA rms noise in a bandwidth of 5-kHz (eight-pole Bessel filter). This could then be a significant source of noise to the overall measurement. On the other hand, a 10-MΩ pipette with a 10-fF patch would produce only about 6-fA rms of noise in this bandwidth. The most extreme situation

that we are aware of is that reported by Benndorf[10] in which pipettes with resistances on the order of 50–100 MΩ (tip diameter ~0.2 μm) were used to form patches with a capacitance that should typically be less than 1 fF. Such a patch and pipette would produce less than 2-fA rms noise in a 5-kHz bandwidth. Either of the last two examples clearly produces noise that is negligible in comparison to other sources of noise associated with the pipette. Thus in most cases R_e-C_p noise is easy to make sufficiently small to be ignored. Of course, with giant patches that can have capacitances significantly greater than 1 pF, R_e-C_p noise can become a very important, often dominant, source of noise. Even though the resistance of the large-tipped pipettes used in giant-patch recordings is much less than that of more "typical" patch pipettes, the increased patch capacitance more than makes up for this in terms of noise. Thus, for a large-tipped pipette with R_e = 100 kΩ and C_p = 10 pF, R_e-C_p noise is expected to be more than 0.7-pA rms in a 5-kHz bandwidth. In such cases, however, the signals being measured are usually relatively large and thus higher noise levels can be tolerated.

SEAL NOISE. The *minimum* noise of a gigaseal is readily determined as its expected thermal current noise. This would produce a PSD of $4kT/R_{sh}$, where R_{sh} is the *DC* seal resistance, and an rms noise given by $(4kTc_1B/R_{sh})^{1/2}$. Seals can range from a few gigohms up to as much as 4 TΩ (4×10^{12} Ω). Thus, a seal with a resistance of only 2 GΩ would produce a minimum of about 0.2-pA rms noise for a 5-kHz bandwidth while a 4-TΩ seal would produce a minimum of only about 5-fA rms in this bandwidth. It is clear that high-resistance seals are a prerequisite for very low noise patch-clamp recordings. Unfortunately, however, it is not clear that the noise associated with a seal is well described by its minimum thermal current noise. We have presented evidence that the noise of at least some seals (resistance range 40–100 GΩ) is indistinguishable from the thermal current noise expected on the basis of the seal resistance.[9] However, it certainly seems that seal noise can often exceed this minimum amount.

More generally, the expected PSD of the membrane–glass seal for zero applied voltage should be given by $4kT\,\mathrm{Re}\{Y_{sh}\}$, where $\mathrm{Re}\{Y_{sh}\}$ is the real part of the seal admittance. The minimum value of $\mathrm{Re}\{Y_{sh}\}$ is $1/R_{sh}$. Of course, the measured "seal resistance" is actually the parallel combination of the seal and the patch membrane (with all known channels closed). In most situations we do not expect that the membrane itself will contribute much to the measured resistance (e.g., a 10-fF patch with a specific resistance of 20 kΩcm^2 would have a resistance of 2 TΩ), but the membrane contribution to apparent seal noise should be remembered, and it should be borne in mind that the membrane may also contain other charge translocating processes that may be thought of as contributing to what would commonly

be called seal noise. In any case, the noise of the seal/patch may very well exceed the minimum estimate described earlier. Because noise often varies in unexplained ways from one patch to the next (even when all measured parameters seem similar) it is tempting to blame such variations on the seal. This seems particularly reasonable since noise measured with pipettes sealed to Sylgard is generally quite consistent and in good agreement with theoretical predictions. On the other hand, noise from actual patches shows much more variation (although general trends are as expected, see, e.g., Levis and Rae[8]). The only difference between a pipette sealed to Sylgard and an actual patch should be the seal/patch; other sources of pipette noise should be the same in both cases. Thus, it frequently seems reasonable (if anecdotal) to attribute noise variations in membrane patches to unexplained differences in the seal/patch.

Benndorf[10] has suggested that seals may produce shot noise. Shot noise is associated with current flow across a potential barrier. We know of no obvious reason to expect shot noise to be generated by the seal, although since the precise nature of the membrane–glass seal is not known, shot noise cannot be ruled out.

Despite the uncertainties in regard to seal noise it is clear that it is minimized by high-resistance seals. Benndorf[10] has reported that very small tipped pipettes (opening diameter ~0.2 μm) resulting in tiny patches can produce seals in the range of 1–4 TΩ. He also suggests that seal resistance should be linearly inversely related to pipette pore diameter. We have certainly noticed a correlation between small-tipped pipettes and high-resistance seals, but it is not altogether precise. We have frequently obtained seals with resistances in the range of 100–200 GΩ with pipettes with resistances of ~5 MΩ. Extremely high resistance seals should be of considerable importance to noise minimization at low to moderate bandwidths (provided, of course, that the electronics used can take advantage of such low noise at these frequencies). Thus, for example, with the amplifier considered here, and a 1-TΩ seal, total noise at bandwidths of 100 Hz and 1 kHz could be as little as 2- and 9-fA rms, respectively (of course, somewhat higher values are more likely in most cases). As bandwidth increases the contribution of seal noise to total noise will decrease because the rms value of seal noise should vary with bandwidth as $B^{1/2}$, whereas rms dielectric noise will vary as B, and distributed RC noise and R_c-C_p noise (as well as much of the noise of the amplifier) will produce rms noise that varies as $B^{3/2}$.

The simplest strategy for obtaining high-resistance seals and thereby minimizing seal noise is to use relatively small-tipped pipettes. The size of the tip, of course, will also be dependent on the type of measurement being undertaken (e.g., when studying channels with a low density in the cell membrane, very small tipped pipettes can become quite frustrating). Seal

noise may sometimes be as low as the predicted thermal current noise of the DC seal resistance, but it certainly seems that it can frequently exceed this lower limit.

SUMMARY AND STRATEGIES. At this point it is useful to summarize the noise sources described and to provide an indication of the magnitudes of these noises that can be expected in "typical" low-noise recording situations and in "best case" situations. The total rms noise, i_T, of a single-channel patch-clamp recording in a particular bandwidth can be summarized as

$$i_T = (i_{hs}^2 + i_h^2 + i_d^2 + i_{RC}^2 + i_{ep}^2 + i_{sh}^2)^{1/2} \quad \text{amp rms} \qquad (11)$$

Where i_{hs} is the rms noise of the headstage amplifier, *including* any correlated noise arising from e_n in series with capacitance of the pipette and its holder; i_h is the (uncorrelated) noise of the holder; i_d is the dielectric noise of the pipette; i_{RC} is the distributed RC noise of the pipette; i_{ep} is R_e-C_p noise; and i_{sh} is the noise of the seal, including any noise arising from the patch membrane itself.

Headstage noise obviously depends on the amplifier being used; the noise of the amplifier one of us uses has already been described. The open-circuit noise of this amplifier in a 5-kHz bandwidth (eight-pole Bessel filter) is 41-fA rms. This noise increases to about 44, 47, and 50-fA rms in this bandwidth with the addition of 1, 2, and 3 pF, respectively, of capacitance to the input due to this capacitance in series with e_n. This represents the capacitance of the holder and pipette, but ignores other sources of noise associated with these capacitances.

Holder noise is minimized by using small holders made from low-loss materials (or a small metal holder such as that described by Benndorf[10]). These can be purchased commercially or custom made; in either case the noise performance of the holder should be measured (with and without a pipette with its tip just above the bath) to ensure acceptable results, and its noise should then be monitored periodically. In our experience, custom-made holders can often outperform those that are commercially available. However, holder noise is usually sufficiently small that the added inconvenience of a custom-made holder is normally not necessary. If holder noise increases, the holder must be cleaned. The addition of a small polycarbonate holder with about 0.6 pF of capacitance should add about 15-fA rms of noise in a 5-kHz bandwidth; a larger (~1.5-pF) polycarbonate holder adds about 25-fA rms. Taking into account the capacitance of the holder added to the input, total noise with such holders will increase to about 45- to 46-fA rms for the small holder and about 52-fA rms for the larger holder with the low-noise headstage amplifier considered here.

Pipette noise in general is minimized by using short pipettes (although we have never used extremely short—as little as 8 mm—pipettes such as

those favored by Benndorf[10]) fabricated from thick-walled glass tubing ($d_o/d_i \geq 2$) and heavily coated with a low-loss elastomer as close to the tip as possible. Shallow depths of immersion also minimize pipette noise. Small tip openings are also generally desirable for the lowest noise recordings because this will tend to minimize seal noise and R_e-C_p noise.

In the case of dielectric noise, the best approach to minimization is the use of quartz. However, reasonable results can also be achieved with other low-loss glasses. Regardless of the type of glass used, thick-walled pipettes are desirable as are techniques of pulling that attempt to preserve the d_o/d_i ratio as closely as possible near the tip. Heavily coating the pipette with a low-loss elastomer will reduce the noise of pipettes made from glasses other than quartz, but may actually increase the dielectric noise of a quartz pipette. But note that a very heavy elastomer coating with a quartz pipette is predicted to produce less dielectric noise than a moderate coating—even though both should produce more dielectric noise than is predicted for an uncoated quartz pipette. Even so, quartz pipettes heavily coated with Sylgard 184 or R-6101 have been measured to produce only about half the dielectric noise of similar pipettes made from other glasses. For an ~2-mm depth of immersion dielectric noise of quartz pipettes ($d_o/d_i = 2$ prior to pulling) has been measured to be about 35-fA rms in a 5-kHz bandwidth. For pipettes of essentially the same geometry, elastomer coating, and depth of immersion made from other low-loss glasses, we have typically found that dielectric noise is 70-fA rms or more in this bandwidth. Recalling that dielectric noise varies linearly with bandwidth, these numbers will double for a 10-kHz bandwidth. The rms dielectric noise should vary roughly as the square root of immersion depth and also roughly as the square root of pipette capacitance. With thicker walled glass and shallower depths of immersion dielectric noise can be reduced further. For example, with $d_o/d_i = 4$ quartz and an immersion depth of 500 μm it should be possible to keep dielectric noise to as little as 10-fA rms in a 5-kHz bandwidth. The fact that dielectric noise from elastomer-coated pipettes fabricated from glasses other than quartz exceeds theoretical predictions deserves further investigation.

Distributed *RC* noise is highly dependent on the geometry of the pipette, but almost independent of the type of glass used. Several examples of distributed *RC* noise have already been presented. From these it can be seen that for pipettes of the general geometry that we use most frequently (see Fig. 3), it should be possible in a 5-kHz bandwidth to keep distributed RC noise less than 30-fA rms for an immersion depth of ~2 mm with a moderate to heavy coating of Sylgard 184 (or other suitable low-loss elastomer). With an extremely heavy Sylgard coating it should be possible to reduce distributed RC noise to as little as 15-fA rms under the same

conditions. Thus distributed *RC* noise can be made smaller than dielectric noise even in quartz pipettes at a bandwidth of 5 kHz; for pipettes made from glasses other than quartz (which will have little effect on distributed *RC* noise, but significant effects on dielectric noise) at this bandwidth dielectric noise is likely to exceed distributed *RC* noise of an optimal pipette by a factor of as much as 4–5. Remember, however, that rms distributed *RC* noise will vary with bandwidth (B) as $B^{3/2}$, while dielectric noise varies as B. This means that at lower bandwidths distributed *RC* noise becomes less and less important, while at wider bandwidths distributed *RC* noise becomes progressively more important. If rms distributed *RC* noise is two times smaller than dielectric noise at a 5-kHz bandwidth, it will become equal to rms dielectric noise at a bandwidth of 20 kHz. Thus, the bandwidth of the measurement to be undertaken must also be considered. Fortunately, the steps taken to minimize distributed *RC* noise and dielectric noise are generally the same. The only significant exception to this is the decision whether or not to use quartz. The major advantage of quartz relates to dielectric noise, consequently at very high bandwidths (as well as very low bandwidths where neither dielectric noise or distributed *RC* noise are likely to dominate overall noise) the advantages of quartz over low-loss borosilicates may become unimportant. However, from our experience the bandwidths in question are in excess of 50 kHz.

Distributed *RC* noise is generally minimized by using thick-walled glass (tubing $d_o/d_i \geq 2$), heavy coats of elastomer extending as close to the tip as practical, and shallow depths of immersion. The benefits of very thick walled glass (e.g., $d_o/d_i = 4$) are dependent on the geometry of the pipette and may not be as large as expected in many actual situations. Effects of immersion depth are minimized by very heavy coatings of elastomer.

R_c-C_p noise is usually only expected to become significant relative to other noise sources when C_p is in the range of roughly 0.1 pF or higher. Such patches are sometimes necessary (e.g., when studying channels with a low density in the cell membrane), but can bring with them a noise penalty. In situations where relatively large patches are necessary it is clearly advantageous in terms of R_c-C_p noise to use the lowest resistance pipettes possible. However, for the lowest noise recordings smaller patches are best able to avoid R_c-C_p noise. In a 5-kHz bandwidth, R_c-C_p noise can range from a few fA rms for patches with $\leq$10 fF of capacitance up to perhaps 100-fA rms for patches in the range of 200–300 fF. For giant patches ($C_p > 1$ pF) R_c-C_p noise is likely to dominate overall noise at bandwidths above a few kilohertz (provided of course that other noise sources have been minimized).

The noise of a high-resistance seal is normally most important at low bandwidths (say, a few kilohertz or less). However, as described earlier,

there is reason to suspect that seal noise may be somewhat unpredictable. It has been shown that under some circumstances seal noise cannot be distinguished from the expected thermal current noise of the *DC* seal resistance, R_{sh}. This is the minimum amount of seal noise possible, and amounts to 40-, 20-, and 9-fA rms in a 5-kHz bandwidth for seal resistances of 50, 200, and 1000 GΩ, respectively. Higher noise may well occur for such seal resistances, but it is clear that higher resistance seals produce less noise. Small tip openings tend to produce the highest resistance seals, but we have often obtained seal resistances in the 100- to 200-GΩ range with tip openings of about 1 μm.

It is of some interest to predict what sort of noise can be expected for the best measurements presently possible, as well as what is reasonable to expect in more "typical" low-noise situations. For an eight-pole Bessel filter it is reasonable to approximate best case pipette noise (excluding noise associated with pipette capacitance in series with e_n and also excluding noise of the seal/patch) for a relatively small-tipped (roughly 0.5 μm) quartz pipette with a heavy elastomer coating and a depth of immersion of ~1 mm:

$$\{1.5 \times 10^{-35}B^2 + 2 \times 10^{-39}B^3\}^{1/2} \quad \text{amp rms}$$

where the B term is dielectric noise, and the $B^{3/2}$ term is distributed RC noise and a smaller contribution from R_e-C_p noise. To this noise it is necessary to add the noise of the amplifier (including correlated noise arising from holder and pipette capacitance in series with e_n), the uncorrelated noise of the holder, and the noise of the seal/patch. Since the seal/patch is harder to predict, we begin by adding the noise of the amplifier described earlier and a small low-noise holder. These will contribute roughly the following rms noise (eight-pole Bessel filter is assumed):

$$\{2 \times 10^{-32}B + 3.2 \times 10^{-35}B^2 + 1.1 \times 10^{-38}B^3\}^{1/2} \quad \text{amp rms}$$

Total best case noise is then

$$\{2 \times 10^{-32}B + 4.7 \times 10^{-35}B^2 + 1.3 \times 10^{-38}B^3 + \text{seal/patch noise}\}^{1/2} \quad \text{amp rms}$$

This then predicts a best case noise of the rms addition of 54-fA rms + seal/patch noise for a 5-kHz bandwidth and 134-fA rms + seal/patch noise for a 10-kHz bandwidth. If the seal/patch noise was as little as 20- and 28-fA rms in bandwidths of 5 and 10 kHz, respectively, total noise could be as little as 58- and 137-fA rms in these bandwidths. These values are only very slightly less than the best noise we have ever achieved with real patches.

For a Schott 8330 or 8250 borosilicate pipette of the same general geometry as that shown in Fig. 2 and assuming dielectric noise of 70-fA

rms in a 5-kHz bandwidth, best case noise would increase to about 86- and 188-fA rms in 5- and 10-kHz bandwidths respectively.

"Typical" noise of a quartz or borosilicate patch pipette in a situation where all of the low-noise practices described have been followed and a very high resistance seal has been achieved can be estimated to be perhaps 30–50% higher than the figures just quoted. For seals of roughly 100 GΩ and Sylgard-coated quartz pipettes pulled from $d_o/d_i = 2$ quartz and tip openings of 0.5–1.0 μm, we have found that average noise is about 85- to 90-fA rms in a 5-kHz bandwidth. However, as already noted, it is certainly not an infrequent occurrence to have done everything right, achieved a high-resistance seal, and ended up with noise significantly higher than this. Much of this variability may be due to the seal, but it also seems likely that the other noise factors considered here show significant variation from one patch to the next.

Noise in Whole-Cell Patch-Clamp Measurements

Whole-cell measurements are subject to all of the same noise sources described in regard to single-channel recording situations with the exception of R_e-C_p noise. Of course, R_e-C_p noise is replaced in the whole-cell situation by noise arising from the pipette/access resistance in series with the whole-cell capacitance, C_m. This is a much larger source of noise since the cell capacitance is many times larger than the capacitance of the patch. In the case of R_e-C_p noise the time constant formed by R_e and C_p is sufficiently small to be ignored in almost all patch-clamp situations (R_e-C_p should be on the order of about 1 μs or less in most cases). However, in the whole-cell situation the time constant R_s-C_m (where R_s is the series resistance, normally dominated by the pipette) can be as high as a few milliseconds and is typically on the order of 100–300 μs (e.g., 210 μs for a more or less "typical" 30-pF cell with a total series resistance of 7 MΩ). Note that the series resistance is called R_s even though it is usually dominated by the resistance of the pipette (called R_e throughout this article). This is to distinguish the total access or series resistance from the pipette resistance measured prior to sealing and achieving the whole-cell configuration. Measured series resistance is normally higher than the initial resistance of the pipette. This can result from partial clogging of the pipette tip as well as from other sources of resistance in series with the membrane.

Noise arising from R_s and C_m has a PSD, S_{sm}^2, given by

$$S_{sm}^2 = (4\pi^2 f^2 e_s^2 C_m^2)/(1 + 4\pi^2 f^2 \tau_{sr}^2) \qquad \text{amp}^2/\text{Hz} \qquad (12)$$

where $\tau_{sr} = R_{sr}$-C_m and R_{sr} is the uncompensated portion of the series resistance and $e_s^2 = 4kTR_s$ is the PSD of the thermal voltage noise of R_s.

The fraction of series resistance that is compensated will be denoted by α ($0 < \alpha < 1$) and $\beta = 1 - \alpha$; thus $R_{sr} = \beta R_s$.

Series resistance compensation is very important to the dynamic characteristics of whole-cell voltage clamping as has been described previously (see, e.g., Refs. 16 and 19). The effects of IR drops producing voltage errors are well known and are not discussed here. Instead, the most important point we wish to emphasize (and have described previously on several occasions) is that in the absence of series resistance compensation the actual maximum usable bandwidth of a whole-cell recording is limited to $1/(2\pi\tau_s)$, where $\tau_s = R_s$-C_m. This is because the series resistance and the cell capacitance effectively form a one-pole low-pass RC filter at this frequency. This restriction can be quite severe; for example, with $R_s = 10$ MΩ and $C_m = 100$ pF, $1/(2\pi\tau_s) \approx 160$ Hz. Series resistance compensation increases this maximum usable bandwidth to $1/(2\pi\tau_{sr})$, so that with the same parameters just considered but with 80% series resistance compensation $1/(2\pi\tau_{sr}) \approx 800$ Hz; 90% compensation will extend this to 1600 Hz. Of course, most situations are better than the example just considered, but even with $R_s = 5$ MΩ and $C_m = 30$ pF, $1/(2\pi\tau_s) \approx 1.06$ kHz, and, for example, 65% series resistance compensation is needed to extend the maximum usable bandwidth to 3 kHz. Setting an external filter bandwidth to anything higher than $1/(2\pi\tau_{sr})$ will essentially add no new information, but it will add additional noise. (Of course, this can be corrected after the fact by the use of a digital filter.)

Examination of Eq. (12) shows that the PSD of the noise arising from R_s and C_m will initially rise as f^2 at frequencies below $1/(2\pi\tau_{sr})$ and will then eventually plateau at frequencies above $1/(2\pi\tau_{sr})$. Without series resistance compensation ($R_{sr} = R_s$), the value of the PSD once this plateau is reached will be $4kT/R_s$, which is the thermal current noise of R_s. With R_s compensation the plateau reaches a level given by $4kT/\beta^2 R_s$. This is a quite significant amount of noise, so that it can be seen that there is a sizable noise penalty (with little if any new information about the signal) for setting the external filter to a bandwidth greater than $1/(2\pi\tau_{sr})$.

Below frequencies of about $1/2\pi\tau_{sr}$, Eq. (12) can be approximated by $4\pi^2 f^2 e_s^2 C_m^2$ and the rms noise current arising from R_s and C_m is then given by $\{(4/3)\pi^2 c_3 e_s^2 C_m^2 B^3\}^{1/2}$, which (noting that $e_s^2 = 4kTR_s$) can also be written as $\{1.33\pi^2 c_3 (4kTR_s) C_m^2 B^3\}^{1/2}$. To consider a more or less typical example, we assume that $R_s = 7$ MΩ and $C_m = 30$ pF and that enough series resistance compensation is used to justify any bandwidths mentioned. This will produce rms noise of approximately 0.15, 1.6, 8.5, and 18.3 pA in bandwidths

[19] A. Marty and E. Neher, *in* "Single Channel Recording" (B. Sakmann and E. Neher, eds.), 2nd Ed., p. 31. Plenum, New York and London, 1995.

(eight-pole Bessel filter) of 200 Hz, 1 kHz, 3 kHz, and 5 kHz respectively. All of these values are much higher than the noise described earlier for the amplifier plus pipette, even when the fact that the amplifier for whole-cell measurements normally uses a 500-MΩ feedback resistor is taken into account. Whole-cell amplifiers typically have noise of less than 0.2-pA rms in a 1-kHz bandwidth and less than 0.5-pA rms in a 5-kHz bandwidth. Because of the increased noise of the patch clamp itself, and more importantly the noise resulting from R_s and C_m, the characteristics of the pipette are clearly much less critical to the noise performance in whole-cell situations. Even with a very favorable situation for low-noise whole-cell recording it can be appreciated that the noise of R_s in series with C_m should still dominate total noise at bandwidths above about 1 kHz. As an example of such a favorable situation consider R_s = 5 MΩ and C_m = 10 pF. In this case the noise from R_s and C_m will be about 0.46- and 5.2-pA rms in bandwidths of 1 and 5 kHz, and exceeds the rms current noise of a 500-MΩ resistor at all bandwidths above about 390 Hz.

Despite these conclusions it seems wise to continue to follow good low-noise practices even with whole-cell pipettes. This would include using low melting temperature glasses with reasonably low dissipation factors (Schott 8250 is a good selection) and at least a light to moderate coat of a suitable elastomer. Among other things this will minimize the size of the pipette capacity transient and especially reduce the amplitude of the slow component of this transient (see Rae and Levis[7]). However, thick-walled glass is usually unnecessary (and may be detrimental, see later discussion), and we doubt that quartz will find significant use in fabricating whole-cell pipettes. The most important characteristic of the pipette in terms of noise in whole-cell situations is its resistance, which normally dominates R_s. This is because of the role it plays in producing noise in conjunction with C_m. In the range of bandwidths below $1/(2\pi\tau_{sr})$ it can be seen that rms noise arising from R_s and C_m depends linearly on C_m and on $R_s^{1/2}$. Reducing either R_s or C_m will reduce noise, but in general C_m is not under the experimenter's control. Besides, if you are studying a particular channel type with a density per unit membrane area that is constant among cells of different sizes, then it is clear that the signal as well as the rms R_s-C_m noise will both scale linearly with C_m, so that in this situation signal-to-noise ratio does not depend on C_m. Thus, in most cases the only practical way of reducing noise (and increasing signal-to-noise ratio) is to minimize R_s, and this means minimizing R_e.

In most situations it is advantageous to use pipettes with tip openings as large as can conveniently form seals with the cells you are using. In addition, it is beneficial to pull pipettes with relatively large cone angles. This is often most easily accomplished by pulling pipettes with quite large

tips prior to heat polishing and then using heat polishing to achieve the desired final opening diameter.[7] Thin-walled tubing often makes this process easier, and as already noted the penalties in terms of dielectric and distributed *RC* noise of the pipette are generally unimportant in whole-cell situations.

Thus, in terms of achieving low noise, the best strategy for whole-cell recording is to use relatively large-tipped pipettes with large cone angles. It is also important to remember that the bandwidth of the measurement should not normally exceed $1/(2\pi\tau_{sr})$ since such unnecessary bandwidths will simply add noise without adding significant new information.

Conclusion

This article has attempted to describe both theoretical and practical aspects of noise reduction for single-channel and whole-cell patch-clamp recordings. In the case of single-channel (small patch) measurements it has been shown that the most important sources of noise arising from the pipette can be sufficiently minimized so that even the quietest electronics presently available can still dominate total noise.

For whole-cell measurements, minimizing the resistance of the pipette (which normally dominates total series resistance) is the best way to reduce noise and to ensure a good signal-to-noise ratio.

Low-noise measurements can require some patience and some perseverance, but there is nothing magic about achieving the levels of performance we have described in this article. The best of results are relatively infrequent (for reasons that are not altogether clear), but very good results can become more or less routine. The techniques described and the understanding of the noise sources that we have attempted to provide are the first steps toward achieving such results. The habits formed in ensuring the best possibility of low-noise measurements are good ones and should improve the quality of patch-clamp measurements in general.